Preparation of primary standard mixtures for atmospheric oxygen measurements with less than 1 µmol mol^{-1} uncertainty for oxygen molar fractions

Nobuyuki Aoki[1], Shigeyuki Ishidoya[2], Nobuhiro Matsumoto[1], Takuro Watanabe[1], Takuya Shimosaka[1], and Shohei Murayama[2]

[1]National Meteorology Institute of Japan, National Institute of Advanced Industrial Science and Technology (AIST), Tsukuba, 305-8563, Japan

[2]National Institute of Advanced Industrial Science and Technology (AIST), Tsukuba, 305-8569, Japan

Correspondence to: Nobuyuki Aoki (aoki-nobu@aist.go.jp)

Abstract. Precise monitoring of changes in atmospheric O_2 levels was implemented by preparing primary standard mixtures with less than 1 µmol mol^{-1} standard uncertainty for O_2 molar fractions. In this study, these mixtures were crafted in 10 L high-pressure aluminium alloy cylinders using a gravimetric method in which unknown uncertainty factors were theoretically determined and subsequently reduced. Molar fractions of the constituents (CO_2, Ar, O_2, and N_2) in the primary standard mixtures were mainly resolved using masses of the respective source gases (CO_2, Ar, O_2, and N_2) that had been filled into the cylinders. To precisely determine the masses of the source gases, the difference in mass of the cylinder before and after filling the respective source gas was calculated by compared with an almost identical reference cylinder. Although the masses of the cylinders filled with source gas with respect to the reference cylinder tended to deviate in relation to temperature differences between the source gas filled cylinder and surrounding air, the degree of the deviation could be efficiently reduced by measuring the two cylinders at the exact same temperature. The standard uncertainty for the cylinder mass obtained in our weighing system was determined to be 0.82 mg. The standard uncertainties for the O_2 molar fractions in the primary standard mixtures ranged from 0.7 µmol mol^{-1} to 0.8 µmol mol^{-1}. Based on the primary standard mixtures, the annual average molar fractions of atmospheric O_2 and Ar in 2015 at Hateruma Island, Japan, were found to be 209339.1 ± 1.1 µmol mol^{-1} and 9334.4 ± 0.7 µmol mol^{-1}, respectively. The molar fraction for atmospheric Ar was in agreement with previous reports.

1 Introduction

Observation of atmospheric O_2 molar fractions provides important information about the global carbon cycle (Keeling and Shertz, 1992; Bender et al., 1996; Keeling et al., 1996, 1998a; Stephens et al., 1998; Battle et al., 2000; Manning and Keeling, 2006). For example, long-term observation allows the estimation of land biotics and oceanic CO_2 uptake (Manning and Keeling, 2006; Tohjima et al., 2008; Ishidoya et al., 2012a, 2012b). Various measurement techniques have been developed for this purpose, including the utilization of interferometry (Keeling et al., 1998b), mass spectrometry (Bender et al., 1994; Ishidoya et al., 2003; Ishidoya and Murayama, 2014), a paramagnetic technique (Manning et al., 1999; Aoki et al., 2018; Ishidoya et al., 2017), a vacuum-ultraviolet absorption technique (Stephens et al., 2003), gas chromatography (Tohjima, 2000), and a method utilizing fuel cells (Stephens et al., 2007; Goto et al., 2013). In all these cases, calibration using standard mixtures is required to precisely determine the relationship between the analysis output and O_2 molar fractions obtained.

Molar fractions of O_2 and Ar are commonly expressed as functions of the O_2/N_2 and Ar/N_2 ratios relative to an arbitrary reference (Keeling and Shertz, 1992; Keeling et al., 2004) in per meg (one per meg is equal to 1×10^{-6}).

2 $$\delta(O_2/N_2) \ = \ \frac{[n(O_2)/n(N_2)]_{sam}}{[n(O_2)/n(N_2)]_{ref}} - 1 \qquad\qquad (1)$$

4 $$\delta(Ar/N_2) \ = \ \frac{[n(Ar)/n(N_2)]_{sam}}{[n(Ar)/n(N_2)]_{ref}} - 1 \qquad\qquad (2)$$

8 In these equations, n depicts the amount of each substance, and the subscripts "sam" and "ref" refer to sample air and reference

9 air, respectively. As the O_2 and Ar molar fractions in air are 20.946% and 0.943%, respectively, a respective change of 4.8

10 per meg and 107 per meg in $\delta(O_2/N_2)$ and $\delta(Ar/N_2)$ corresponds to a change of 1 $\mu mol\ mol^{-1}$ in molar fractions of O_2 and Ar.

11 Reported peak-to-peak amplitudes of seasonal cycles and trends in atmospheric $\delta(O_2/N_2)$ were within the range of 50 – 150

12 per meg (10 – 30 $\mu mol\ mol^{-1}$ for O_2 molar fractions) and −20 per meg yr^{-1} (−4 $\mu mol\ mol^{-1}\ yr^{-1}$ for O_2 molar fractions)

13 (Keeling et al., 1993; Battle et al., 2000; Van der Laan–Luijkx et al., 2013). To monitor these slight variations, the development

14 of primary standard mixtures with standard uncertainty of less than 5 per meg for O_2/N_2 ratios (1 $\mu mol\ mol^{-1}$ for O_2 molar

15 fractions) or less (Keeling et al., 1993; WMO, 2016) is required. In this study, the primary O_2 standard mixture with the

16 recommended uncertainty of 5 per meg (1 $\mu mol\ mol^{-1}$) or less is hereafter referred to as a "highly precise O_2 standard mixture

17 (HPO)".

18 In general, standard mixtures need to be prepared in which molar fractions of the greenhouse gas species, such as CO_2, CH_4,

19 and N_2O, are stable enough during the observation period to enable monitoring of long-term changes in atmospheric molar

20 fractions of their species. For this purpose, it is indispensable to establish methods for determining absolute molar fractions

21 of greenhouse gases in the standard mixtures with required precision. Approved primary standard mixtures exist for CO_2, CH_4,

22 and N_2O, prepared by manometry (Zhao et al., 1997) or gravimetry (Tanaka et al., 1983; Matsueda et al., 2004; Dlugokencky

23 et al., 2005; Hall et al., 2007). However, preparing an HPO is challenging since it is necessary to prepare it with the relative

24 uncertainty of less than one-fifth of that for the CO_2 molar fraction in the CO_2 standard mixture. Since there is no common

25 scale for atmospheric O_2 observation, such as the ratio of O_2/N_2 determined using HPOs, each laboratory has employed

26 reference air determined using its own reference scale instead of a universal scale. This reference scale is determined based

27 on O_2/N_2 ratios in primary standard mixtures filled in high-pressure cylinders and is considered to be sufficiently stable during

28 the observation period (e.g. Keeling et al., 1998b; Tohjima et al., 2008; Ishidoya et al., 2012b). However, there are many

29 deterioration risks of the O_2/N_2 ratio in aluminium cylinders used for reference air and the primary standard mixtures. these

30 include fractionations of O_2 and N_2 induced by pressure, temperature and water vapor gradients (Keeling et al., 1998b),

31 adsorption/desorption of the constituents on the inner surface (Leuenberger et al., 2015), and permeation/leakage of the

32 constituents from/through the valve (Sturm et al., 2004; Keeling et al., 2007). In order to avoid these risks, the cylinders are

33 handled in accordance to certain best practices, including orienting cylinders horizontally to minimize thermal and

34 gravitational fractionation (Keeling, et al. 2007, Leuenberger, et al., 2015).

35 Although causes behind the fractionation should be sufficiently described by now, the effects of permeation and

36 adsorption/desorption have not been completely understood in the long-term scale. To enable comparison of O_2/N_2 values

1 reported based on reference air with the difference scale directly, an independent development of primary standard mixtures

2 with standard uncertainty of 5 per meg (1 μmol mol^{-1}) or less is needed. In a pioneering study, Tohjima et al. (2005) first

3 prepared primary standard mixtures for the atmospheric O_2 measurement based on a gravimetric method. The standard

4 uncertainties for the O_2/N_2 ratio (the O_2 molar fraction) were noted at 15.5 per meg (2.9 μmol mol^{-1}), which was larger than

5 the required standard uncertainty of 5 per meg (1 μmol mol^{-1}) or less. Since the 2.9 μmol mol^{-1} standard uncertainty recorded

6 by Tohjima et al. (2005) was significantly larger than the gravimetrically expected value of 1.6 μmol mol^{-1}, it was suggested

7 that there are unknown factors exerting influence on the mass results of cylinders.

8 Taking these facts into consideration, in this study we set out to develop a new gravimetric method to prepare an HPO by

9 scientifically understanding the unknown uncertainty factors in the cylinder mass measurement. Our laboratory has built upon

10 the weighing system proposed by Matsumoto et al. (2004), in which gravimetry was used to prepare standard mixtures.

11 Although this system allows accurate mass measurements with a standard uncertainty of 2.6 mg, this proves insufficient to

12 prepare an HPO. A new mass comparator with better repeatability was recently introduced to the weighing system. In the

13 present study, we theoretically identified the unknown factors and presented an improved means of minimizing them. The

14 standard uncertainties for molar fractions of all constituents in HPOs, prepared using these improved means, are discussed.

15 Moreover, the molar fractions of all constituents in the HPOs were validated by comparing the gravimetric value with the

16 measured values of CO_2 mole fraction, Ar/N_2 ratio, and O_2/N_2 ratio. In order to validate the scale of O_2/N_2 ratio at the National

17 Institute of Advanced Industrial Science and Technology (AIST) determined using the HPOs prepared in this study, the annual

18 average of O_2/N_2 ratios in 2015 at Hateruma Island (24°03′N, 123°49′E, Japan) obtained from our measurements of air samples

19 were preliminarily compared with the annual average of O_2/N_2 ratios in 2015 at Hateruma Island on the NIES scale determined

20 by Tohjima et al.(NIES). Additionally, the molar fractions for atmospheric Ar and O_2 in air samples were determined using

21 the HPOs and compared with previously reported values.

22 **2 Materials and Methods**

23 **2.1 Preparation of the highly precise O_2 standard mixtures**

24 Eleven HPOs were prepared in 10 L aluminium alloy cylinders (Luxfer Gas Cylinders, UK), with a diaphragm valve (G-55,

25 Hamai Industries Limited, Japan) with poly(chlorotrifluoroethylene) (PCTFE) as sealant in accordance with ISO 6142-1:2015.

26 Pure CO_2 (>99.998 %, Nippon Ekitan Corporation, Japan), pure Ar (G1-Grade, 99.9999 %, Japan Fine Products, Japan), pure

27 O_2 (G1-Grade, 99.99995 %, Japan Fine Products, Japan), and pure N_2 (G1-Grade, 99.99995 %, Japan Fine Products, Japan)

28 were used as source gases to prepare the HPOs. The value of $\delta^{13}C$ in pure CO_2 (which was adjusted to the atmospheric level)

29 was −8.92‰ relative to Vienna Pee Dee Belemnite (VPDB). Impurities in the source gases were identified and quantified

30 using gas chromatography with a thermal conductivity detector for N_2, O_2, CH_4 and H_2 in pure CO_2, and gas chromatography

31 with a mass spectrometer for O_2 and Ar in pure N_2 and N_2 in pure O_2. A Fourier transform infrared spectrometer was used for

32 detection of CO_2, CH_4 and CO in pure N_2, O_2, and Ar. A galvanic cell-type O_2 analyser was employed to quantify O_2 in pure

33 Ar. A capacitance-type moisture meter measured H_2O in pure CO_2, and a cavity ring-down-type moisture meter measured

34 H_2O in pure N_2, O_2 and Ar.

35 Primarily, standard mixtures of CO_2 in Ar were prepared by combining pure CO_2 and pure Ar using a gravimetric method.

36 The molar ratios of CO_2 to Ar were close to the atmospheric molar ratio of CO_2 (400 μmol mol^{-1} or 420 μmol mol^{-1}) to Ar

1 (9340 μmol mol^{-1}). The 10 L aluminium cylinder was used to prepare the HPO after evacuation by a turbomolecular pump.

2 The source gases were filled in the order of the mixtures of CO_2 in Ar, pure O_2 and pure N_2 in a filling room where the

3 temperature was controlled at 23 ± 1 ℃ and humidity was not regulated. The mass of the CO_2 in Ar standard mixture filled

4 was determined by the difference in the mass of the cylinder before and after filling with the mixture. The masses of the filled

5 pure O_2 and N_2 were treated in the same manner. The final pressure in the cylinder was 12 MPa, and masses of the individual

6 gases were approximately 18 g of CO_2 in Ar standard mixture, 300 g of pure O_2, and 1000 g of pure N_2.

7 **2.2 Weighing procedure for a cylinder**

8 The masses obtained for the cylinders were determined using the same weighing system as reported by Matsumoto et al.

9 (2004), except for the mass comparator. The mass comparator used in the study of Matsumoto et al. was replaced with a new

10 mass comparator (XP26003L, Mettler Toledo, Switzerland), which had a maximum capacity of 26.1 kg, a sensitivity of 1 mg,

11 and a linearity of 20 mg. In this study, a cylinder whose mass was measured is hereafter referred to as a "sample cylinder".

12 Mass measurement for sample cylinders was performed in a weighing room where temperature and humidity were controlled

13 at 26 ± 0.5 ℃ and 48 ± 1 %, respectively. The temperature, humidity, and atmospheric pressure surrounding our weighing

14 system were measured using a USB connectable logger (TR-73, T and D Corporation, Japan).

15 Mass measurements of the sample cylinder were conducted with respect to an almost identical reference cylinder aiming to

16 reduce any influence exerted by zero-point drifts, sensitivity issues associated with the mass comparator, changes in buoyancy

17 acting on the cylinder, and/or adsorption effects on the cylinder surface due to the presence of water vapor (Alink et al., 2000;

18 Milton et al., 2011). This is carried out according to several consecutive weighing operations in the ABBA order sequence,

19 where "A" and "B" denote the reference cylinder and the sample cylinder, respectively. The process of loading and unloading

20 of the cylinders was automated. One complete cycle of the ABBA sequence required five minutes. The "mass reading"

21 recorded by our weighing system was given as the difference between both cylinders mass readings, which was obtained by

22 subtracting the reference cylinder reading from the sample cylinder reading.

23 Because the output of mass comparators is generally known to be nonlinear, there is a tendency to under- or over-estimate

24 mass readings for the sample cylinders in our weighing system. This is because the relation between the output of mass

25 comparators and the mass of artefacts tend to be different among various scale ranges. To reduce the influence of this

26 nonlinearity, sample cylinders were weighed only when the difference in readings between the sample and reference cylinders

27 was less than 500 mg. This was achieved by placing standard weights on a weighing pan alongside the sample or reference

28 cylinder. Any mass differences obtained in our weighing system took into account the masses and buoyancies of the standard

29 weights. The masses of the standard weights were traceable to the International System of Units. The standard uncertainties

30 of the masses were 0.25 mg, 0.045 mg, 0.028 mg, 0.022 mg, 0.018 mg, 0.014 mg, 0.011 mg, and 0.0090 mg for the 500 g,

31 100 g, 50 g, 20 g, 10 g, 5 g, 2 g, and 1 g weights, respectively.

32 Temperatures of the sample and reference cylinders were alternately measured by a thermocouple-type thermometer with a

33 resolution of 0.1 K (TX1001 digital thermometer, probe-90030, Yokogawa Test and Measurement Corporation, Tokyo, Japan)

34 before and after weighing of the cylinders.

1 **2.3 Determination procedure of isotopic abundances for O and N**

2 Each HPO was prepared using pure O_2 from two 48 L cylinders and pure N_2 from three or four 48 L cylinders as source gases.

3 The isotopic abundances (^{16}O, ^{17}O, ^{18}O, ^{14}N, and ^{15}N) for pure O_2 and N_2 may be different between cylinders, resulting in

4 abundance differences among each HPO. The averaged values of isotopic abundances in pure O_2 (two cylinders) and pure N_2

5 (three or four cylinders) used for the respective HPOs were calculated based on the ratios of $^{18}O/^{16}O$, $^{17}O/^{16}O$, and $^{15}N/^{14}N$ in

6 the HPOs. These were calculated using the equations, $^{18}O/^{16}O = [\delta(^{18}O/^{16}O) + 1] \times (^{18}O/^{16}O)_{ref}$, $^{17}O/^{16}O = [\delta(^{17}O/^{16}O) + 1] \times$

7 $(^{17}O/^{16}O)_{ref}$, and $^{15}N/^{14}N = [\delta(^{15}N/^{14}N) + 1] \times (^{15}N/^{14}N)_{ref}$. The terms $\delta(^{17}O/^{16}O)$, $\delta(^{18}O/^{16}O)$, and $\delta(^{15}N/^{14}N)$ which were

8 determined by a mass spectrometer (Delta-V, Thermo Fisher Scientific Inc., USA) represent the deviation from the

9 corresponding atmospheric value (Ishidoya and Murayama, 2014). The isotopic ratios of $\delta(^{17}O/^{16}O)$, $\delta(^{18}O/^{16}O)$, and

10 $\delta(^{15}N/^{14}N)$ were approximately equal to those of $\delta(^{17}O^{16}O/^{16}O^{16}O)$, $\delta(^{18}O^{16}O/^{16}O^{16}O)$, and $\delta(^{15}N^{14}N/^{14}N^{14}N)$, since

11 $^{17}O^{17}O/^{16}O^{16}O$, $^{18}O^{18}O/^{16}O^{16}O$ and $^{15}N^{15}N/^{14}N^{14}N$ tended to be much less than $^{17}O^{16}O/^{16}O^{16}O$, $^{18}O^{16}O/^{16}O^{16}O$ and

12 $^{15}N^{14}N/^{14}N^{14}N$. Values of $(^{18}O/^{16}O)_{ref}$, $(^{17}O/^{16}O)_{ref}$, and $(^{15}N/^{14}N)_{ref}$ refer to ratios of $^{18}O/^{16}O$, $^{17}O/^{16}O$, and $^{15}N/^{14}N$ in reference

13 air. In the present study, natural air in a 48 L aluminium cylinder (Cylinder No. CRC00045), equipped with a diaphragm valve

14 (G-55, Hamai Industries Limited, Japan) was used as reference air in the AIST scale (hereafter referred to AIST reference

15 air). The AIST reference air was prepared in 2011 by filling natural air into the cylinder to a pressure of about 13 MPa after

16 drying cryogenically by using a highly efficient water trap at the dew point temperature lower than -80 °C (Ishidoya and

17 Murayama, 2014). It has been confirmed that the $\delta(O_2/N_2)$ on the AIST scale is higher by several hundred per meg than that

18 on the Scripps Institution of Oceanography (SIO) scale (e.g. Manning and Keeling, 2006) by reflecting the difference of the

19 filling years of the respective references for AIST and SIO scales (Ishidoya et al., 2016). The corresponding atmospheric

20 values shown in Table 1 were used as the ratios of $(^{17}O/^{16}O)_{ref}$, $(^{18}O/^{16}O)_{ref}$, and $(^{15}N/^{14}N)_{ref}$, as isotopic abundances in the

21 troposphere are considered to be constant (Junk and Svec, 1958; Baertschi, 1976; Li et al., 1988; Barkan and Luz, 2005).

22 Because differences between isotopic ratios of N_2, O_2, Ar in the AIST reference air and air samples at Hateruma were

23 sufficiently small to be negligible, their fractionations due to preparation of the AIST reference air are ignored.

24 **2.4 Analytical methods**

25 In this study, a mass spectrometer was used to determine O_2/N_2 and Ar/N_2 ratios in the HPOs. A cavity ring-down spectrometer

26 was used to examine consistency among molar fractions of CO_2 in the HPOs. In this section, we describe the analytical

27 methods and relationships between the absolute O_2/N_2 (Ar/N_2) ratios and the mass-spectrometry based isotopic ratios.

28 **2.4.1 Evaluations of O_2/N_2 and Ar/N_2 ratios in highly precise O_2 standard mixtures and natural air**

29 Ratios of O_2/N_2 and Ar/N_2 in the HPOs were validated by comparison of gravimetrically calculated values with the measured

30 values obtained by the mass spectrometer (Delta-V, Thermo Fisher Scientific Inc., USA). The mass spectrometer was adjusted

31 to measure ion beam currents for masses 28 ($^{14}N^{14}N$), 29 ($^{15}N^{14}N$), 32 ($^{16}O^{16}O$), 33 ($^{17}O^{16}O$), 34 ($^{18}O^{16}O$), 36 (^{36}Ar), 40 (^{40}Ar),

32 and 44 ($^{12}C^{16}O^{16}O$) simultaneously. Isotopic ratios of $\delta(^{15}N^{14}N/^{14}N^{14}N)$, $\delta(^{17}O^{16}O/^{16}O^{16}O)$, $\delta(^{18}O^{16}O/^{16}O^{16}O)$,

33 $\delta(^{16}O^{16}O/^{14}N^{14}N)$, $\delta(^{36}Ar/^{40}Ar)$, and $\delta(^{40}Ar/^{14}N^{14}N)$ were determined against the AIST reference air using the mass

34 spectrometer. In our prepared HPOs, the ratios of $\delta(O_2/N_2)_{HPO\_grav}$ and $\delta(Ar/N_2)_{HPO\_grav}$, comprised of all isotopes of O_2, N_2

35 and Ar and gravimetrically calculated, are not equal to the isotopic ratios of $\delta(^{16}O^{16}O/^{14}N^{14}N)_{HPO\_meas}$ and

1 $\delta(^{40}\text{Ar}/^{14}\text{N}^{14}\text{N})_{\text{HPO\_meas}}$ measured by the mass spectrometer. This is because the isotopic ratios in source gases are different

2 from the corresponding atmospheric values. The subscripts "HPO_grav" and "HPO_meas" hereafter refer to the gravimetric

3 value and the measured value in the HPO. Thus, mass-spectrometry based isotopic ratios need to be converted to values

4 equivalent to the $\delta(\text{O}_2/\text{N}_2)_{\text{HPO\_grav}}$ ratio and the $\delta(\text{Ar}/\text{N}_2)_{\text{HPO\_grav}}$ ratio. The values of $\delta(\text{O}_2/\text{N}_2)_{\text{HPO\_meas}}$ and $\delta(\text{Ar}/\text{N}_2)_{\text{HPO\_meas}}$ were

5 calculated using mass-spectrometry based on isotopic ratios $^{15}\text{N}^{14}\text{N}/^{14}\text{N}^{14}\text{N}$, $^{17}\text{O}^{16}\text{O}/^{16}\text{O}^{16}\text{O}$, $^{18}\text{O}^{16}\text{O}/^{16}\text{O}^{16}\text{O}$, $^{36}\text{Ar}/^{40}\text{Ar}$, and

6 $^{38}\text{Ar}/^{40}\text{Ar}$ as depicted in equations (3) and (4). Isotopic species of $^{17}\text{O}^{17}\text{O}$, $^{18}\text{O}^{17}\text{O}$, $^{18}\text{O}^{18}\text{O}$, $^{15}\text{N}^{15}\text{N}$, were negligible because the

7 abundance of these species was very small.

9 $\delta(\text{O}_2/\text{N}_2)_{\text{HPO\_meas}} = \left[\delta(^{16}\text{O}^{16}\text{O}/\,^{14}\text{N}\,^{14}\text{N})_{\text{HPO\_meas}} + 1\right] \times$

10 $\left[\frac{1+^{17}\text{O}^{16}\text{O}/^{16}\text{O}^{16}\text{O}+^{18}\text{O}^{16}\text{O}/^{16}\text{O}^{16}\text{O}}{1+^{15}\text{N}\,^{14}\text{N}/^{14}\text{N}^{14}\text{N}}\right]_{\text{HPO}} \Big/ \left[\frac{1+^{17}\text{O}^{16}\text{O}/^{16}\text{O}^{16}\text{O}+^{18}\text{O}^{16}\text{O}/^{16}\text{O}^{16}\text{O}}{1+^{15}\text{N}\,^{14}\text{N}/^{14}\text{N}^{14}\text{N}}\right]_{\text{ref}} - 1$ (3)

12 $\delta(\text{Ar}/\text{N}_2)_{\text{HPO\_meas}} = \left[\delta(^{40}\text{Ar}/\,^{14}\text{N}^{14}\text{N})_{\text{HPO\_meas}} + 1\right] \times \left[\frac{1+^{36}\text{Ar}/^{40}\text{Ar}+^{38}\text{Ar}/^{40}\text{Ar}}{1+^{15}\text{N}\,^{14}\text{N}/^{14}\text{N}^{14}\text{N}}\right]_{\text{HPO}} \Big/ \left[\frac{1+^{36}\text{Ar}/^{40}\text{Ar}+^{38}\text{Ar}/^{40}\text{Ar}}{1+^{15}\text{N}\,^{14}\text{N}/^{14}\text{N}^{14}\text{N}}\right]_{\text{ref}} - 1$

13   (4)

15 The values of $^{15}\text{N}^{14}\text{N}/^{14}\text{N}^{14}\text{N}$, $^{17}\text{O}^{16}\text{O}/^{16}\text{O}^{16}\text{O}$, and $^{18}\text{O}^{16}\text{O}/^{16}\text{O}^{16}\text{O}$ in the HPOs and the AIST reference air were calculated using

16 isotope abundances of O and N determined by the procedure described in section 2.3 (Table 1). The $^{36}\text{Ar}/^{40}\text{Ar}$ ratio of pure

17 Ar filled in the HPOs was calculated using equation $^{36}\text{Ar}/^{40}\text{Ar} = [\delta(^{36}\text{Ar}/^{40}\text{Ar})_{\text{HPO\_meas}} + 1] \times (^{36}\text{Ar}/^{40}\text{Ar})_{\text{ref}}$. The

18 $\delta(^{36}\text{Ar}/^{40}\text{Ar})_{\text{HPO\_meas}}$ value was determined by mass spectrometry of the HPOs. The $(^{36}\text{Ar}/^{40}\text{Ar})_{\text{ref}}$ value obtained was the

19 atmospheric value ($^{36}\text{Ar}/^{40}\text{Ar} = 0.003349 \pm 0.000004$), because isotopic abundances of Ar in the AIST reference air were

20 equal to that of the atmospheric value. The value of $^{38}\text{Ar}/^{40}\text{Ar}$ in the HPOs and the AIST reference air, which could not be

21 measured, was assumed to be $^{38}\text{Ar}/^{40}\text{Ar} = 0.000631 \pm 0.000004$ taken from previous reports as the atmospheric values.

22 Deviations of respective abundances of ^{38}Ar from the atmospheric value were considered to be less than the uncertainty of the

23 atmospheric value for ^{38}Ar. The atmospheric values of isotopic abundances for Ar were reported in an IUPAC technical report

24 (Böhlk, 2014).

25 On the other hand, the absolute O_2/N_2 ratio in the AIST reference air was calculated by substituting the $(\text{O}_2/\text{N}_2)_{\text{HPO\_grav}}$ in the

26 HPOs and the $\delta(\text{O}_2/\text{N}_2)_{\text{HPO\_meas}}$ for $(\text{O}_2/\text{N}_2)_{\text{sam}}$ and for $\delta(\text{O}_2/\text{N}_2)$ in equation (1). The absolute Ar/N_2 ratio in the AIST reference

27 air was calculated in same manner (see the section 5.3).

28 **2.4.2 Measurements of CO_2 in highly precise O_2 standard mixtures**

29 Molar fractions of CO_2 in HPOs were verified using a cavity ring-down spectrometer (G2301, Picarro Inc., USA) equipped

30 with a multi-port valve (Valco Instruments Co. Inc., USA) for gas introduction and a mass flow controller (SEC-N112,

31 100SCCM, Horiba STEC, CO., Ltd, Japan). The cavity ring-down spectrometer was calibrated by three primary standard

32 gases ($364.50 \pm 0.14\ \mu\text{mol mol}^{-1}$, $494.04 \pm 0.14\ \mu\text{mol mol}^{-1}$, and $500.32 \pm 0.14\ \mu\text{mol mol}^{-1}$) that had been prepared from pure

33 CO_2 and purified Air (G1 grade, Japan Fine Products, Japan) in accordance with ISO 6142-1:2015. The individual standard

34 gases were continuously measured for 30 minutes, respectively and the data last ten minutes were used. The pure CO_2 was

35 the same as the source gas used for preparation of the HPOs.

3 Identifying and minimizing unknown factors of uncertainty

As previously mentioned,, there are several unknown factors that influence mass readings obtained for sample cylinders. Identifying and minimizing these unknown factors is discussed in this section.

3.1 Factors to cause deviations of mass readings

Generally, mass readings of a sample cylinder obtained from a mass comparator tend to vary due to numerous factors such as buoyancy, adsorption/desorption and thermal effects. The buoyancy effect is caused by changes in the density of the surrounding air due to variations in ambient temperature, humidity, and pressure. Adsorption effect can greatly influence mass readings of a sample cylinder by adsorption and desorption of water vapor from surrounding ambient air on the external surface of a sample cylinder (Alink et al., 2000; Mizushima, 2004, 2007; Milton et al., 2011). The thermal effect is related to temperature gradients between a sample cylinder and the surrounding ambient air (Gläser, 1990, 1999; Mana et al., 2002; Gläser and Borys, 2009; Schreiber et al., 2015), which is able to change the weight force of the sample cylinder through frictional forces exerted on the vertical surface of a sample cylinder and pressure forces on the horizontal surface. Both the friction and pressure forces are caused by the upward or downward flow of air that is heated or cooled, respectively, by the sample cylinder.

When the ABBA technique is employed for mass measurements under identical experimental conditions, the deviations of the mass readings due to the factors described above become negligible because they are equally exerted on both the sample and the reference cylinder. In fact, the buoyancy effect could be cancelled by adopting the ABBA technique in our mass measurements (see Section 4.3.1). On the other hand, the identical experimental conditions tend to be disturbed by the temperature change on the sample cylinder surface by adiabatic compression of the source gases and by the temperature difference between the filling room and the weighing room. Mass readings of the sample cylinder deviate from true values when thermal effects due to a change in the sample cylinder surface temperature are exerted independently and at varying degrees on the sample and reference cylinders. Moreover, the amount of water adsorbed on the sample cylinder surface can also be influenced by humidity if the level in the filling room is different from that in the weighing room. This non-uniformity of temperatures and the water amount between the sample cylinder surface and the surrounding ambient air is assumed to be the main contributor of uncertainties in obtained mass readings of the sample cylinder (Matsumoto et al., 2008). In order to identify and minimize the contribution to the non-uniformity, we examined the equilibrium of both humidity and temperature for the surface of the sample cylinder used in this study before carrying out any measurement.

3.2 Identifying and minimizing unknown uncertainty factors

Equilibrium in the temperature and the water amount between the sample cylinder surface and its surrounding ambient air is considered to be achieved by placing the sample cylinder on our weighing system for an appropriate duration of time before the mass reading. Here, the equilibrium between the reference cylinder surface and its surrounding ambient air is always achieved as the reference cylinder is permanently left on the weighing system. The equilibrium for the sample cylinder is easily disturbed by the processes of its evacuation and filling of the source gases. To quantify the appropriate time interval needed to restore equilibrium, the mass readings of the sample cylinder were recorded after the evacuation and after the filling. These values were plotted against the time elapsed after evacuation and filling (Figure 1). The surface temperature of the

sample cylinder recorded after the evacuation was 2 K lower, while the temperatures recorded after the filling for CO_2 in Ar standard mixture, pure O_2, and pure N_2 were −0.7 K, 1 K, and 6 K higher than that of the reference cylinder, respectively. In this experiment, the equilibria were considered to be achieved when the standard deviation of the mass readings remained constant for two or more hours with the repeatability value of < 0.82 mg (see in Section 4.3.1.). Interestingly, the mass readings recorded after the evacuation and filling for CO_2 in Ar mixture tended to decrease as time elapsed, while those after filling with pure O_2 and N_2 gases tended to increase. Deviations in mass readings had some connection with the temperature difference between the reference and sample cylinders. The results imply that warmer cylinders appear lighter.

Appropriate time intervals were defined as the time elapsed from the evacuation or the filling time to the point of re-achieving equilibrium. This time interval was noted as 5 h after complete evacuation. Time intervals required after filling with relevant gases were different depending on the filled gas species to some extent. For the CO_2 in Ar mixture, equilibria were achieved in 3 h to 5 h, while 4 h to 5 h were required for O_2 equilibration and 7 h to 9 h for N_2. These intervals indicate that preparation of a single HPO requires several days. To determine the mass of the sample cylinder in as short time as possible, a clear indicator for carrying out mass measurement is needed.

As described above, the deviations in mass readings are considered to have some relation with the temperature differences in the sample and reference cylinders. Therefore, we proceeded to examine this relationship to understand whether the temperature difference can be the indicator. The closed squares shown in Figure 2 indicate that the deviation of mass readings was proportional to temperature differences. This deviation rate was determined to be −14.3 mg K^{-1}. Although the results indicate that a temperature difference of 0.1 K causes a deviation of 1.4 mg, the deviation in the recorded mass readings ensures the repeatability value of 0.82 mg that is achieved by reducing the temperature difference to below 0.06 K. By conducting measurements of the cylinder temperature using the thermocouple-type thermometer and ensuring that the mass readings were taken when the temperature of both cylinders were the same, we were able to reduce the deviation contributing to the mass readings.

To validate the proposed weighing procedure, the reproducibility of mass readings obtained after disturbing the equilibrium was measured. Hence, the mass reading sequence after a cooling or heating cycle of the cylinders was examined. Figure 3 illustrates the results in which four heating cycles (number 1 to 4) and four cooling cycles (number 5 to 8) were conducted. In this experiment, temperatures of the cooled or heated cylinder were 1 K to 3 K lower or 10 K to 20 K higher than that of the reference cylinder, respectively. When mass readings were recorded after ensuring equal temperatures of both the sample and reference cylinders, no difference in mass readings recorded after the cooling and heating cycles was detected. The reproducibility of mass readings was estimated to be 0.44 mg with regards to the standard deviation of the mass readings shown in Figure 3. The fact that reproducibility was lower than the repeatability value validated the weighing procedure. The contributions to mass readings by non-equilibrium conditions were negligible using the established weighing procedure.

It is difficult to determine whether deviations in mass readings recorded for sample cylinders were caused by thermal or adsorption effects simply by analysing these results. This is because both effects are related to temperature fluctuations. However, the thermal effect influenced the slope of the calibration function solely through temperature differences, whereas the adsorption/desorption effect influenced the slope of the calibration function via a combination of both ambient temperature and humidity. This is because the adsorbed or desorbed amounts of water on the surface of both cylinders are highly dependent on the cylinder temperature and humidity of the surrounding ambient air. To determine which of these effects contributed the

1   most to the deviations, the relationship between the deviations and temperature differences was investigated under various

2   conditions in the weighing room. Humidity was stringently controlled at 30%, 50%, 65%, and 80%, whereas temperature

3   levels were maintained at 22 °C, 26 °C, and 29 °C. As shown in Figure 2, the slope did not depend on the humidity nor

4   temperature. These results indicate that the dominant factor of deviations in mass readings was rather an effect of thermal

5   gradients than adsorption, because the deviations depended on the temperature difference only. Therefore, we focused on

6   minimizing the impact of any thermal gradient in further experiments.

7   **4 Evaluation of uncertainty factors for the O_2 Standard Mixtures**

8   In this section, we discuss any uncertainty factors associated with molar fractions of constituents in the HPOs. The gravimetric

9   molar fraction (y_k) of the constituent k (CO_2, Ar, O_2, and N_2) was calculated using the molar mass (M_i) and the molar fraction

10   ($x_{i,j}$) of the constituent i (CO_2, Ar, O_2, N_2 and impurities) in the filled source gas j (CO_2 in Ar standard mixture, pure O_2, and

11   pure N_2). Additionally, mass (m_j) of the source gases filled into the sample cylinder were incorporated into equation (5) in

12   accordance with ISO 6142-1:2015.

14   $$y_k = \frac{\sum_{j=1}^{r}\left(\frac{x_{k,j}\times m_j}{\sum_{i=1}^{q} x_{i,j}\times M_i}\right)}{\sum_{j=1}^{r}\left(\frac{m_j}{\sum_{i=1}^{q} x_{i,j}\times M_i}\right)} \qquad (5)$$

16   In this equation, r and q represent the number of source gases j and constituents i, respectively, while $x_{k,j}$ is the molar fraction

17   of the constituent k in the source gas j. Uncertainties ($u(y_k)$) associated with the gravimetric molar fraction were calculated

18   according to the law of propagation.

20   $$u^2(y_k) = \sum_{j=1}^{r}\sum_{i=1}^{q}\left(\frac{\partial y_k}{\partial x_{i,j}}\right)^2 \times u^2(x_{i,j}) + \sum_{i=1}^{q}\left(\frac{\partial y_k}{\partial M_i}\right)^2 \times u^2(M_i) + \sum_{j=1}^{r}\left(\frac{\partial y_k}{\partial m_j}\right)^2 \times u^2(m_j) \qquad (6)$$

22   In this equation, $u(A)$ depicts the standard uncertainty for A. Gravimetric molar fractions of the constituent k and its associated

23   uncertainty in the molar fractions for the HPOs prepared in this study were calculated using equation (5) and equation (6),

24   and they are listed in Table 2. The standard uncertainties for the constituents N_2, O_2, Ar, and CO_2 were 0.8 – 1.0 μmol mol^{-1},

25   0.7 – 0.8 μmol mol^{-1}, 0.6 – 0.7 μmol mol^{-1}, and 0.03 μmol mol^{-1}, respectively. Table 3 lists the contribution of the purity of

26   the source gases, molar masses of the constituents, and masses of the source gases to the gravimetric molar fraction. These

27   correspond to the square root of the first, second, and third terms found in equation (6), respectively. Uncertainty factors in

28   the gravimetric molar fractions in the HPOs were mainly those of the mass for the source gases filled into the sample cylinder.

29   Contributions from other sources of uncertainty were negligible. Purity of the source gases and molar masses of the

30   constituents i, as well as the masses of the source gases and their associated standard uncertainties, are described in Sections

31   4.1, 4.2, and 4.3.

4.1 Purity of source gas

Pure O_2, N_2, Ar, and CO_2 were used as source gases to prepare the HPOs. Molar fractions of impurities presented in source gases and their associated standard uncertainties were determined based on the primary standard gases prepared in accordance with ISO 6142-1:2015. When the molar fraction of impurity h was under its detection limit (L_h), the molar fraction (x_h) and standard uncertainty ($u(x_{h,\,j})$) of h in the source gas j was calculated using the equations $x_{h,j} = L_{h,j}/2$ and $(x_{h,j}) = L_{h,j}/2\sqrt{3}$. The calculated values for the impurities and purities of the source gases are listed in Table 4.

4.2 Molar masses of constituents

Molar masses (M_i) of the constituents were calculated using most recent atomic masses and isotopic abundances reported by the IUPAC. However, IUPAC values for atomic masses of O and N have large standard uncertainties because they reflect variability present in individual isotopic abundances of natural terrestrial matter. Using IUPAC values, standard uncertainties for N_2 and O_2 molar fractions in the HPOs were calculated to be 4 μmol mol^{-1}. In addition, atmospheric values of their isotopic abundances could not be used for calculating molar masses of the source gases even though pure O_2 and N_2 were produced from air. This is because isotopically abundant O and N in pure O_2 and N_2 tends to deviate from the corresponding atmospheric value during the production process. Therefore, the isotopic abundances of O and N in HPOs were precisely determined using mass spectrometry. Their isotopic abundance and associated standards of uncertainty are shown in Table 1. The difference of isotopic abundances of O and N between respective HPOs were negligible.

Based on the isotopic abundances obtained in this study and the atomic masses of O and N in the filled source gases, pure O_2 and N_2 were determined with relative standard uncertainties of 0.000029 % and 0.000006 %, respectively. It was shown that the uncertainty in molar masses is negligible (Table 3). Although the grade and supplier of the pure O_2 and N_2 used in this study were the same as those of the source gases used by Tohjima et al. (2005), the atomic masses (15.999366 (1) for O and 14.006717 (4) for N) obtained for the two elements were different from Tohjima et al. reported values (15.999481 (8) for O and 14.006677 (4) for N). These differences resulted in a deviation of 0.4 μmol mol^{-1} and 1.2 μmol mol^{-1} for O_2 and N_2, respectively. Since these results infer that the ratios of O and N isotopes change with production time, the isotopic abundances of O and N in the source gases have to be precisely determined whenever HPOs are prepared using different pure O_2 and N_2. On the other hand, standard uncertainties in the atomic mass presented in an IUPAC technical report by De Laeter et al. (2003) were sufficient for further use in the case of Ar and CO_2 as source gases.

4.3 Determining the masses of the filled gases

Masses of individual gases that were filled into the sample cylinders were calculated using the mass difference before and after the filling. The standard uncertainty of the obtained mass was calculated by combining standard uncertainties of mass readings of the sample cylinder before and after filling each gas. To determine uncertainty in mass reading of the sample cylinder, three factors were evaluated i.e., the repeatability $u(m_{rep})$ of the mass readings, permeation $u(m_{gas\ permeate})$ of the source gases during weighing, and buoyancy change $u(m_{buoyancy})$ due to the expansion of the cylinder. The standard uncertainties ($u(m_{cyl})$) were defined according to equation (7).

1     $u^2(m_{cyl}) = u^2(m_{rep}) + u^2(m_{gas\ permeate}) + u^2(m_{buoyancy}).$ (7)

3 These factors are discussed in detail in sections 4.3.1, 4.3.2, and 4.3.3. The standard uncertainties of masses for the individual

4 filled gases were 1.2 mg regardless of the gas species.

5 **4.3.1 Repeatability of mass readings**

6 The repeatability of mass readings was evaluated by continuous mass measurement of sample cylinders using the ABBA

7 technique over three days. This is because preparation of a single HPO requires three days. Mass readings were recorded after

8 the sample cylinder was left on the weighing system for at least a week. Air density was likewise measured for three days by

9 carefully monitoring temperature, humidity, and pressure changes in ambient air (Figure 4). Our findings indicate that the

10 mass readings remain stable during the three-day experiment. The standard deviation of mass readings (0.82 mg) is

11 represented as repeatability $u(m_{rep})$. The fact that the mass readings were not affected by changes in the air density also

12 indicates that buoyancy issues influencing the sample cylinder were cancelled out by changes simultaneously affecting the

13 reference cylinder.

14 **4.3.2 Permeation of source gases during weighing**

15 All of the cylinders used in this study have diaphragm valves, which were joined to the cylinders via pipe fittings and sealed

16 with Teflon tape. The seal of diaphragm valves was made from PCTFE, through which gases tend to permeate quite slowly

17 (Sturm, 2004). Since permeation of the source gases during weighing the sample cylinders resulted in evaluation error of the

18 masses for the source gases, we examined the permeability of purified air by monitoring mass of the sample cylinder filled

19 with purified air at a pressure of 8 MPa. The changes in mass readings were measured for over four months. From these results,

20 it was determined that the permeability was 0.013 mg day^{-1}. This effect was considered to be negligible because it is much

21 lower than the repeatability. Therefore, the contribution of permeability ($u(m_{gas\ permeate})$) to the standard uncertainty

22 calculations ($u(m_{cyl})$) was ignored. On the other hand, the amount of air permeating from the sample cylinder during the

23 course of a year was calculated to be about 4.7 mg. This quantity may cause changes in the composition of the HPO if the

24 mixture is kept for extended periods of time, since the gas permeability depends on the gas species (Sturm, 2004).

25 **4.3.3 Buoyancy effect of cylinder expansion**

26 Oh et al. (2013) reported that volume in the 10 L aluminium cylinders linearly increases with increase in internal pressure,

27 and volume expansion was determined to be 24 ± 2 ml when the pressure difference in the sample cylinders was 12 MPa.

28 Tohjima et al. (2005) likewise reported a volume expansion of 22 ± 4 ml when the pressure difference was 10 MPa. In this

29 study, we adopted a volume expansion of the sample cylinders as 55 ± 5 ml, measured by a cylinder supplier, when the

30 pressure difference was 25 MPa. Compared to the expansion rate with respect to pressure variations reported by Oh (2.0 ± 0.2

31 ml MPa^{-1}) (2013) and Tohjima (2.2 ± 0.4 ml MPa^{-1}) (2005), expansion rate of the sample cylinders used in this study was

32 determined to be 2.2 ± 0.2 ml MPa^{-1}. The pressure difference recorded before and after filling with source gases was 0.12

33 MPa, 2.5 MPa, and 9.4 MPa for CO_2 in Ar standard mixture, pure O_2, and pure N_2, respectively. These pressure differences

34 were subsequently used to calculate buoyancy effects, which were reported as 0.3 mg, 6.4 mg, and 23.9 mg for CO_2 in Ar

1   standard mixture, pure O_2, and pure N_2, respectively. In turn, these buoyancy effects caused changes in the gravimetric molar

2   fraction of $+0.5$ μmol mol^{-1} and -0.5 μmol mol^{-1} for O_2 and N_2, respectively. The final mass readings were corrected to take

3   these changes into account. The standard uncertainties $u(m_{buoyancy})$ in linear expansion were considered to be negligible.

5 Validation of the constituents in the highly precise O_2 standard mixtures

5   The O_2 molar fractions in the HPOs deviate from gravimetric values with deviation of the molar fractions of other constituents.

6   In this section, the molar fractions of all constituents were validated. The gravimetric and measured values for the CO_2 molar

7   fractions were compared, along with the values of $\delta(Ar/N_2)_{HPO\_grav}$, $\delta(Ar/N_2)_{HPO\_meas}$, $\delta(O_2/N_2)_{HPO\_grav}$ and $\delta(O_2/N_2)_{HPO\_meas}$ to

8   validate the molar fractions of Ar, O_2 and N_2 in the HPOs. Table 5 shows the $\delta(O_2/N_2)_{HPO\_meas}$ and $\delta(Ar/N_2)_{HPO\_meas}$ values

9   calculated using equation (3) and (4), as well as the values for $\delta(^{15}N^{14}N/^{14}N^{14}N)_{HPO\_meas}$, $\delta(^{17}O^{16}O/^{16}O^{16}O)_{HPO\_meas}$,

10    $\delta(^{18}O^{16}O/^{16}O^{16}O)_{HPO\_meas}$, $\delta(^{16}O^{16}O/^{14}N^{14}N)_{HPO\_meas}$, $\delta(^{36}Ar/^{40}Ar)_{HPO\_meas}$, and $\delta(^{38}Ar/^{40}Ar)_{HPO\_meas}$.

5.1 Determining the absolute (O_2/N_2) and (Ar/N_2) ratios in AIST reference air

12   The absolute $(O_2/N_2)_{HPO\_grav}$ and $(Ar/N_2)_{HPO\_grav}$ ratios, as well as the $\delta(O_2/N_2)_{HPO\_meas}$ and $\delta(Ar/N_2)_{HPO\_meas}$ values of the HPOs

13   are listed in Table 2 and Table 5. Using these values, the absolute ratios for O_2/N_2 and Ar/N_2 in AIST reference air were

14   0.2680929 ± 0.0000016 and 0.0119542 ± 0.0000009, respectively. On the AIST scale, these values corresponded to $\delta(O_2/N_2)$

15    $= 0$ and $\delta(Ar/N_2) = 0$. Associated standard uncertainties were determined with regards to the law of propagation of uncertainty.

16   The HPOs prepared in this study did not include minor components of Ne, He, Kr, CH_4, H_2 and N_2O which are present in air

17   samples. Therefore, the variation of the $\delta(^{15}N^{14}N/^{14}N^{14}N)$, $\delta(^{17}O^{16}O/^{16}O^{16}O)$, $\delta(^{18}O^{16}O/^{16}O^{16}O)$, $\delta(^{16}O^{16}O/^{14}N^{14}N)$, $\delta(^{36}Ar/^{40}Ar)$,

18   and $\delta(^{40}Ar/^{14}N^{14}N)$ values obtained by the measurement of mass spectrometry was examined when molar fractions of Ne

19   change from 0 μmol mol^{-1} to 500 μmol mol^{-1}. Consequently, the isotopic ratios did not change significantly depending on

20   Ne. Since abundance of Ne is highest in minor components, the changes of the molar fractions of other minor components

21   also might fail to affect the isotopic ratios measured in this study.

5.2 CO_2 molar fractions and Ar/N_2 ratio

23   Three primary standard gases were used to measure CO_2 molar fractions in HPOs. Table 2 illustrates the gravimetric and

24   measured values and associated standard uncertainties. The CO_2 molar fractions in the cylinder labelled CPB28679, which

25   had been prepared on 29 March 2017, were not measured. Differences between the gravimetric and measured values (obtained

26   by subtracting the measured value from gravimetric value) were found to range from -0.17 μmol mol^{-1} to 0.03 μmol mol^{-1}.

27   The gravimetric values were in line with the measured values, both being within the accepted levels of uncertainty.

28   From these results, mass of the CO_2 in Ar standard mixture which we evaluated were considered validated. Figure 5 shows

29   the plot of the $\delta(Ar/N_2)_{HPO\_meas}$ values relative to the $\delta(Ar/N_2)_{HPO\_grav}$ values, as well as the residuals of the $\delta(Ar/N_2)_{HPO\_meas}$

30   values that had been estimated using the best fitted line by the least squares method. The standard deviation of the residuals

31   was 78 per meg. This standard deviation represents a scatter in the $(Ar/N_2)_{HPO\_grav}$ values, since the standard uncertainty for

32    $\delta(Ar/N_2)_{HPO\_meas}$ was much smaller than the obtained standard deviation (Ishidoya and Murayama, 2014). The standard

33   uncertainties for $\delta(Ar/N_2)_{HPO\_grav}$ values ranged from 65 per meg to 77 per meg. Standard uncertainties were comparable to

1 the standard deviations obtained for the residuals, supporting the validity of uncertainty calculations for the constituents, Ar
2 and N_2.

5.3 O_2/N_2 ratio

4 Figure 5 shows a plot of the $\delta(O_2/N_2)_{HPO\_meas}$ values listed in Table 5 against the $\delta(O_2/N_2)_{HPO\_grav}$ values listed in Table 2, as
5 well as residuals from the fitted line by the least squares method. The slope of the fitted line was determined to be $1.00162 \pm$
6 0.00029, which indicated that the discrepancy between change rates of the $\delta(O_2/N_2)_{HPO\_meas}$ values and the $\delta(O_2/N_2)_{HPO\_grav}$
7 values was within 0.16%. The standard deviation of the residuals was 3.6 per meg, which proved to be in line with the standard
8 uncertainties for the corresponding gravimetric values since the standard uncertainties for the values of $\delta(O_2/N_2)_{HPO\_grav}$ ranged
9 from 3.2 per meg to 4.0 per meg. The agreement with the gravimetric and measured values reinforced the idea that the method
10 for calculating the uncertainties of the constituents, O_2 and N_2, was proper and accurate. On the other hand, the $\delta(O_2/N_2)_{HPO\_meas}$
11 values were lower than their $\delta(^{16}O^{16}O/^{14}N^{14}N)_{HPO\_meas}$ counterparts by 18.2 per meg to 27.1 per meg (Table 5) and differences
12 were larger than the standard uncertainties obtained for both values. This means that the $\delta(O_2/N_2)$ values in the HPOs should
13 be expressed by $\delta(O_2/N_2)_{HPO\_meas}$ rather than $\delta(^{16}O^{16}O/^{14}N^{14}N)_{HPO\_meas}$.
14 The O_2/N_2 ratio of gases delivered from the cylinders may differ from the gravimetric O_2/N_2 ratio by either homogeneous or
15 inhomogeneous fractionation (Leuenberger et al., 2015 Langenfelds et al., 2005 Keeling et al., 2004). In this study, we used
16 the same type of valves and cylinders as in the study of Tohjima et al. (2005). Tohjima et al. examined changes in the O_2/N_2
17 ratio of the HPOs by releasing the inner air into a room at a flow rate of 8 mL min^{-1} and found that the fractionation of O_2 and
18 N_2 during air release was negligible. Therefore, we chose not to evaluate fractionation in this study.

6 Comparison with Previous Values

20 To confirm the consistency of the results obtained using the HPOs, we preliminarily compared O_2/N_2 ratios on both the AIST
21 and NIES scale using annual average of $\delta(O_2/N_2)$ values in the air sample from Hateruma Island collected from January to
22 December in 2015. Additionally, the molar fraction of atmospheric O_2 and Ar were determined based on the HPOs and then
23 compared with previously reported values to confirm consistency of the results.

6.1 Comparison between O_2/N_2 ratios on the AIST and NIES scales

25 We observed the atmospheric $\delta(O_2/N_2)$ by analysing air samples collected at Hateruma Island from January to December in
26 2015. For the air samples, we confirmed that the isotopic ratios of N_2 and O_2 did not differ significantly from the atmospheric
27 values, such that we regard the $\delta(^{16}O^{16}O/^{14}N^{14}N)$ value measured by the mass spectrometer is equivalent to $\delta(O_2/N_2)$ in
28 equation (1). Twice a month, the air samples were collected in two Pyrex glasses arranged in series (one for AIST and the
29 other for NIES). Using these air samples, we determined that the annual average of $\delta(O_2/N_2)$ in 2015 on the AIST scale was
30 -63 ± 3 per meg. The number following the symbol $\pm$ denotes the standard uncertainty of the measurement. Using equation
31 (1), the $\delta(O_2/N_2)$ value on the AIST scale was then converted to the absolute O_2/N_2 ratio by utilizing the absolute ratio of
32 O_2/N_2 in AIST reference air determined in section 5.1. In 2015, the absolute O_2/N_2 ratio on Hateruma Island was 0.2680761
33 ± 0.0000018. This value can be converted to the corresponding $\delta(O_2/N_2)$ value on the NIES scale using equation (1), since
34 the absolute O_2/N_2 ratio in NIES reference air was reported to be 0.2681708 by Tohjima et al. (2005). The converted $\delta(O_2/N_2)$

1   value, which is expressed as δ(O$_2$/N$_2$) $_{\text{NIES on AIST}}$ in the following descriptions, was found to be −353 ± 6 per meg on the NIES

2   scale. The uncertainty expresses the 95% confidence interval.

3   On the other hand, the annual average of δ(O$_2$/N$_2$) in Hateruma island in 2015 measured by NIES on the NIES scale was -395

4   ± 5 per meg (Tohjima, Y., personal communications). The number following the symbol ± denotes the standard uncertainty

5   of the measurement (Tohjima et al., 2008). The δ(O$_2$/N$_2$) value is expressed as δ(O$_2$/N$_2$)$_{\text{NIES on NIES}}$. There was a difference of

6   41 per meg between both values of δ(O$_2$/N$_2$)$_{\text{NIES on AIST}}$ and δ(O$_2$/N$_2$)$_{\text{NIES on NIES}}$. This difference falls outside of the 95%

7   confidence interval. The disagreement between δ(O$_2$/N$_2$)$_{\text{NIES on AIST}}$ and δ(O$_2$/N$_2$)$_{\text{NIES on NIES}}$ suggests that there are some

8   inconsistencies between the gravimetric methods developed by Tohjima et al. (2005) and this study. Additionally, other

9   sources of error may exist (e.g. difference between instruments, sampling method, introduction method). Therefore, a direct

10   comparison of the O$_2$/N$_2$ ratio or the O$_2$ molar fraction between the AIST and NIES scales, by a round-robin experiment of

11   the HPOs developed in this study, is required some time in the near future to quantify the differences in absolute values and

12   span of each gravimetric scale.

13   **6.2 Determination of atmospheric O$_2$ and Ar molar fractions and comparison with previous data**

14   The molar fractions for atmospheric O$_2$ and Ar were determined based on δ(O$_2$/N$_2$) and δ(Ar/N$_2$) values for air samples taken

15   at Hateruma Island in 2015. The δ(O$_2$/N$_2$) and δ(Ar/N$_2$) values were −62.8 per meg and −62.8 per meg, respectively. Using

16   the (O$_2$/N$_2$)$_{\text{ref}}$ and (Ar/N$_2$)$_{\text{ref}}$ ratios for AIST reference air, the δ(O$_2$/N$_2$) and δ(Ar/N$_2$) values were used to calculate the O$_2$/N$_2$

17   and Ar/N$_2$ ratios using equation (1) and (2). In 2015, the calculated O$_2$/N$_2$ and Ar/N$_2$ ratios for samples from Hateruma Island

18   were 0.2680761 ± 0.0000018 and 0.0119534 ± 0.0000009, respectively. The molar fractions of O$_2$ and Ar (x_{O_2} and x_{Ar}) were

19   calculated using the aforementioned O$_2$/N$_2$ and Ar/N$_2$ ratios by using the equations below.

21   $$x_{O_2} = K \times \frac{O_2/N_2}{(1+O_2/N_2+Ar/N_2)} \tag{8}$$

22   $$x_{Ar} = K \times \frac{Ar/N_2}{(1+O_2/N_2+Ar/N_2)} \tag{9}$$

24   In these two equations, K is the sum of N$_2$, O$_2$, and Ar molar fractions in the air samples and was estimated to be 999567.8 ±

25   0.1 μmol mol^{-1}. To obtain this value, the molar fractions of Ne (18.18 μmol mol^{-1}), He (5.24 μmol mol^{-1}), CH$_4$ (1.82 μmol

26   mol^{-1}), Kr (1.14 μmol mol^{-1}), H$_2$ (0.52 μmol mol^{-1}), N$_2$O (0.32 μmol mol^{-1}), CO (0.15 μmol mol^{-1}) and Xe (0.09 μmol mol^{-1})

27   reported by Tohjima et al. (2005) and CO$_2$ (404.7 μmol mol^{-1}) in 2015 were used. The CO$_2$ molar fraction was the average

28   CO$_2$ molar fraction measured using a mass spectrometer. The calculated O$_2$ and Ar molar fractions were 209339.1 ± 1.1 μmol

29   mol^{-1} and 9334.4 ± 0.7 μmol mol^{-1}, respectively. Standard uncertainties were estimated in accordance with the law of

30   propagation of uncertainties. In 2000, Tohjima et al. (2005) reported the atmospheric Ar molar fraction of 9333.2 ± 2.1 μmol

31   mol^{-1} (2005), whereas the value reported for air samples collected on Korea's Anmyeon Island in 2002 and at Niwot Ridge

32   in 2001 was 9332 ± 3 μmol mol^{-1} (Park et al., 2004). Hence, our values for atmospheric Ar were in line previous reports.

7 Conclusion

In this study, we demonstrated that the deviation of mass readings of the sample cylinders is susceptible to temperature differences between the sample and reference cylinders. The contribution degree of the temperature difference was -14.3 mg K^{-1}. Our results also indicate that variations in mass readings due to temperature difference could be reduced to negligible levels by obtaining mass readings at thermal equilibrium. A long time is required to reach thermal equilibrium. Since the variations mainly depend on temperature differences rather than factors related to the adsorption phenomena (e.g., the temperature of the cylinder and/or the humidity of ambient air), it was thus concluded that the variations in mass readings were influenced solely by thermal effects.

We developed a preparation technique for the production of HPOs with atmospheric levels of CO_2, Ar, O_2, and N_2. To determine the O_2 molar fractions with standard uncertainties of less than 1 μmol mol^{-1}, repeatability in measuring the mass readings of the sample cylinders was determined to be 0.82 mg. The impact of leakage or permeation of the source gases through the cylinder valve, as well as change in buoyancy such as the expansion of the cylinder as a factor of the cylinder inner pressure was evaluated. Additionally, the molar masses of the source gases, pure O_2 and pure N_2, were determined based on the abundance of their isotopes. The gravimetrically calculated standard uncertainties were in good agreement with the standard deviation for the corresponding measured values. This indicates that the uncertainty calculations of the gravimetric values for constituents performed in this study were accurate and valid.

Based on the HPOs prepared in this study, we determined molar fractions of atmospheric Ar and O_2 at Hateruma Island in 2015. These values were 9334.4 ± 0.7 μmol mol^{-1} and 209339.1 ± 1.1 μmol mol^{-1}, for Ar and O_2, respectively. The atmospheric Ar molar fraction was in line with the values reported by Park (9332 ± 3 μmol mol^{-1}) and Tohjima (9333.2 ± 2.1 μmol mol^{-1}) (Park et al., 2004; Tohjima et al., 2005).

Acknowledgments

This study was partly supported by funding from the Global Environment Research Coordination System from the Ministry of the Environment, Japan. We express our gratitude to Noritsugu Tsuda, Nobukazu Oda, Fujio Shimano of Global Environmental Forum, and Yasunori Tohjima of National Institute for Environmental Studies for their cooperation in collecting air samples at Hateruma Island.

References

Aoki, N., and Shimosaka, T.: Development of an analytical system based on a paramagnetic oxygen analyzer for atmospheric oxygen variations, *Anal. Sci,* 34, 487–493, 2018.

Alink, A., and Van der Veen, A. M.: Uncertainty calculations for the preparation of primary gas mixtures, *Metrologia*, 37, 641–650, 2000.

Baertschi, P.: Absolute ^{18}O content of standard mean ocean water, *Earth Planet. Sci. Lett.,* 31, 341–344, 1976.

Battle, M., Bender, M. L., Tans, P. P., White, J. W. C., Ellis, J. T., Conway, T., and Francey, R. J.: Global carbon sinks and their variability inferred from atmospheric O_2 and ^{13}C, *Science*, 287, 2467–2470, 2000.

1 Barkan, E. and Luz, B.: High precision measurements of $^{17}O/^{16}O$ and $^{18}O/^{16}O$ ratios in H_2O, *Rapid Commun. Mass Spectrom.,*
2   19, 3737–3742, 2005.

3 Bender, M. L., Tans, P. P., Ellis, J. T., Orchard, J., and Habfast, K.: High precision isotope ratio mass spectrometry method
4   for measuring the O_2/N_2 ratio of air, *Geochim. Cosmochim. Acta.,* 58, 4751–4758, 1994.

5 Bender, M. L., Ellis, J. T., Tans, P. P., Francey, R., and Lowe, D.: Variability in the O_2/N_2 ratio of southern hemisphere air
6   1991–1994: Implications for the carbon cycle, *Global Biogeochem. Cycles*, 10, 9–21, 1996.

7 Böhlk, J. K.: Variation in the terrestrial isotopic composition and atomic weight of argon (IUPAC Technical Report), *Pure*
8   *Appl. Chem.*, 86, 1421−1432, 2014.

9 De Laeter, J. R., Böhlke, J. K., De Bièfre, P., Hidaka, H., Peiser, H. S., Rosman, K. J. R., and Taylor P. D. P.: Atomic weights
10   of the elements: Review 2000 (IUPAC Technical Report), *Pure Appl. Chem.*, 75, 683–800, 2003.

11 Dlugokencky, E. J., Myers, R. C., Lang, P. M., Masarie, K. A., Crotwell, A. M., Thoning, K. W., Hall, B. D., Elkins, J. W.,
12   and Steele, L. P.: Conversion of NOAA atmospheric dry air CH_4 molar fractions to a gravimetrically prepared standard
13   scale, *J. Geophys. Res.*, 110, D18306, doi:10.1029/2005JD006035, 2005.

14 Gläser, M.: Response of apparent mass to thermal gradients, *Metrologia*, 27, 95–100, 1990.

15 Gläser, M.: Change of the apparent mass of weights arising from temperature difference, *Metrologia*, 36, 183–197, 1999.

16 Gläser, M., and Borys, M.: Precision mass measurements, *Rep. Prog. Phys.,* 72, 126101, doi:10.1088/003400.4-
17   4885/72/12/126101, 2009.

18 Goto, D., Morimoto, S., Ishidoya, S., Ogi, A., Aoki, S., and Nakazawa, T.: Development of a high precision continuous
19   measurement system for the atmospheric O_2/N_2 ratio and its application at Aobayama, Sendai, Japan, *J. Meteorol. Soc.*
20   *Japan,* 91, 179–192, 2013.

21 Hall, B. D., Dutton, G. S., and Elkins J. W.: The NOAA nitrous oxide standard scale for atmospheric observations, *J. Geophys.*
22   *Res.*, 112, D09305, doi:10.1029/2006JD007954, 2007.

23 Ishidoya, S., and Murayama, S.:, Development of a new high precision continuous measuring system for atmospheric O_2/N_2
24   and Ar/N_2 and its application to the observation in Tsukuba, Japan, *Tellus B: Chem. Phys. Meteorol.*, 66, 22574, 2014.

25 Ishidoya, S., Aoki, S., and Nakazawa T.: High precision measurements of the atmospheric O_2/N_2 ratio on mass spectrometer,
26   *J. Meteorol. Soc. Japan,* 81, 127–140, 2003.

27 Ishidoya, S., Morimoto, S., Aoki, S., Taguchi, S., Goto, D., Murayama, S., and Nakazawa, T.: Oceanic and terrestrial
28   biospheric CO_2 uptake estimated from atmospheric potential oxygen observed at Ny-Ålesund, Svalbard, and Syowa,
29   Antarctica, *Tellus B: Chem. Phys. Meteorol.*, 64, 18924, 2012a.

30 Ishidoya, S., Aoki, S., Goto, D., Nakazawa, T., Taguchi, S., and Patra, P. K.: Time and space variations of the O_2/N_2 ratio in
31   the troposphere over Japan and estimation of global CO_2 budget, *Tellus B: Chem. Phys. Meteorol.,* 64, 18964, 2012b.

32 Ishidoya, S., Uchida, H., Sasano, D., Kosugi, N., Taguchi, S., Ishii, M., Morimoto, S., Tohjima, Y., Nishino, S., Murayama,
33   S., Aoki, S., Ishijima, K., Fujita, R., Goto, D., Nakazawa, T.: Ship observations of Atmospheric Potential Oxygen and
34   regional air-sea O_2 flux in the Northern North Pacific and the Arctic Ocean, *Tellus B*, 68, 29972, 2016

35 Ishidoya, S., Tsuboi, K., Murayama, S., Matsueda, H., Aoki, N., Shimosaka, T., Kondo, H., and Saito, K.: Development of a
36   continuous measurement system for atmospheric O_2/N_2 ratio using a paramagnetic analyzer and its application on
37   Minamitorishima Island, Japan, *SOL*, 13, 230–234, 2017.

ISO 6142-1:2015, Gas Analysis-Preparation of Calibration Gas Mixtures-Part 1: Gravimetric Method for Class I Mixtures, *International Organization for Standardization*, ISO 6142–1:2015.

Junk, G. A., and Svec, H. J.: The absolute abundance of the nitrogen isotopes in the atmosphere and compressed gas from various sources, *Geochim. Cosmochim. Acta,* 14, 234–243, 1958.

Keeling, R. F., and Shertz, S. R.: Seasonal and interannual variations in atmospheric oxygen and implications for the global carbon cycle. *Nature*, 358, 723–727, 1992.

Keeling, R. F., Bender, M. L., and Tans, P. P.: What atmospheric oxygen measurements can tell us about the global carbon cycle, *Global Biogeochem. Cycles*, 7, 37–67, 1993.

Keeling, R. F., Piper, S. C., and Heimann, M.: Global and hemispheric CO_2 sinks deduced from changes in atmospheric O_2 concentration, *Nature*, 381, 218–221, 1996.

Keeling, R. F., Stephens, B. B., Najjar, R. G., Doney, S. C., Archer, D., and Heimann, M.: Seasonal variations in the atmospheric O_2/N_2 ratio in relation to the kinetics of air-sea gas exchange, *Global Biogeochem. Cycles*, 12, 141–163, 1998a.

Keeling, R. F., Manning, A. C., McEvoy, E. M., and Shertz, S. R.: Methods for measuring changes in atmospheric O_2 concentration and their application in southern hemisphere air, *J. Geophys. Res.* 103, 3381–3397, 1998b.

Keeling, R. F., Blaine, T. Paplawsky, B, Katz, L., Atwood, C., and Brockwell, T.: Measurement of changes in atmospheric Ar/N_2 ratio using a rapid-switching, single-capillary mass spectrometer system, Tellus 56 B, 322-338, 2004

Keeling, R. F., Manning, A. C., Paplawsky, W. J., Cox, A.:On the long-term stability of reference gases for atmospheric O_2/N_2 and CO_2 measurements, *Tellus. 59 B*, 3–14, 2007.

Langenfelds, R. L., Van der Schoot, M. V., Francey, R.J., Steele, L. P. Schmidt, M., and Mukai, H.: Modigication of air standard composition by diffusive and surface processes, *J. Geophys. Res. Atmos.,* 110, D13307, doi:10.101029/2004JD0055482, 2005.

Leuenberger, M. C., Schibig, M. F., and Nyfeler, P.: Gas adsorption and desorption effects on cylinders and their importance for long-term gas records, *Atmos. Meas. Tch.*, 8, 5289-5299, doi:10.5194/amt-8-5289-20158d, 2015.

Li, W., Ni, B., Jin, D., and Chang, T. L.: Measurement of the absolute abundance of oxygen–17 in V–SMOW, *Kexue Tnbao*, 33, 1610–1613, 1988.

Mana, G., Palmisano, C., Perosino, A., Pettorruso, S., Peuto, A., and Zosi, G.: Convective forces in high precision mass measurements, *Meas. Sci. Technol.*, 13, 13–20, 2002.

Manning, A. C., Keeling, R. F., and Severinghaus, J. P.: Precise atmospheric oxygen measurements with a paramagnetic oxygen analyzer, *Global Biogeochem. Cycles,* 13, 1107–1115, 1999.

Manning, A.C., and Keeling, R. F.: Global oceanic and land biotic carbon sinks from the Scripps atmospheric oxygen flask sampling network, *Tellus B: Chem. Phys. Meteorol.*, 58, 95–116, 2006.

Matsueda, H., Sawa, Y., Wada, A., Inoue, H. Y., Suda, K., and Hirano, Y.: Methane standard gases for atmospheric measurements at the MRI and JMA, *Pap. Meteorol. Geophys.*, 54, 91–113, 2004.

Matsumoto, N., Watanabe, T., Maruyama, M., Horimoto, Y., Maeda, T., and Kato, K.: Development of mass measurement equipment using an electronic mass-comparator for gravimetric preparation of reference gas mixtures, *Metrologia,* 41, 178–188, 2004.

Matsumoto, N., Shimosaka, T, Watanabe, T., and Kato, K.: Evaluation of error sources in a gravimetric technique for preparation of a reference gas mixture (carbon dioxide in synthetic air), *Anal. Bioanal Chem.,* 391, 2061–2069, doi: 10.1007/s00216-008-2107-8, 2008.

Milton, M. J. T., Vargha, G. M., and Brown, A. S.: Gravimetric methods for the preparation of standard gas mixtures, *Metrologia*, 48, R1–R9, 2011.

Mizushima, S.: Determination of the amount of gas adsorption on $SiO_2/Si(100)$ surfaces to realize precise mass measurement, *Metrologia*, 41, 137–144, 2004.

Mizushima, S.: The improvement of the adsorption characteristics of stainless steel surfaces by sputter–deposited films, *Metrologia*, 44, 161–166, 2007.

Oh, S. H., Kim, B. M., and Kang, N.: Evaluation of changes in cylinder volume due to gas filling and subsequent release, *Metrologia*, 50, 318–324, 2013.

Park, S. Y., Kim, J. S., Lee, J. B., Esler, M. B., Davis, R. S., and Wielgosz, R. I.: A redetermination of the argon content of air for buoyancy corrections in mass standard comparisons, *Metrologia*, 41, 387–395, 2004.

Schreiber, M., Emran, M. S., Fröhlich, T., Schumacher, J., and Thess, A.: Quantification of free convection effects on 1 kg mass standard, *Metrologia,* 52, 835–841, 2015.

Stephens, B. B., Bakwin, P. S., Tans, P. P., Teclaw, R. M., and Baumann, D.: Application of a differential fuel-cell analyzer for measuring atmospheric oxygen variations, *J. Atmos. Ocean. Technol.*, 24, 82-94, 2007.

Stephens, B.B., Keeling, R. F., Heimann, M., Six, K. D., Mumane, R., and Caldeira, K.: Testing global ocean carbon cycle models using measurements of atmospheric O_2 and CO_2 concentration, *Global Biogeochem. Cycles*, 12, 213–230, 1998.

Stephens, B. B., Keeling, R. F., and Paplawsky, W. J.: Shipboard measurements of atmospheric oxygen using a vacuum-ultraviolet absorption technique, *Tellus B: Chem. Phys. Meteorol.*, 55(4), 857–878, doi: 10.3402/tellusb.v55i4.16386, 2003.

Sturm, P., Leuenberger, M., Sirignano, C., Neubert, R. E. M., Meiger, H. A. J., Langenfelds, R., Brand, W. A., and Tohjima, Y.: Permeation of atmospheric gases through polymer O-rings used in flasks for air sampling, *J. Geophys. Res.*, 109, D04309, 2004.

Tanaka, M., Nakazawa, T., and Aoki, S.: High quality measurements of the concentration of atmospheric carbon dioxide, *J. Meteorol. Soc. Japan,* 61, 678–685, 1983.

Tohjima, Y.: Method for measuring changes in the atmospheric O_2/N_2 ratio by a gas chromatograph equipped with a thermal conductivity detector, *J. Geophys. Res.*, 105, 14575–14584, 2000.

Tohjima, Y., Machida, T., Watai, T., Akama, I., Amari, T., and Moriwaki, Y.: Preparation of gravimetric standards for measurements of atmospheric oxygen and reevaluation of atmospheric oxygen concentration, *J. Geophys. Res.*, 110, D1130, 2005.

Tohjima, Y., Mukai, H., Nojiri, Y., Yamagishi, H., Machida, T.: Atmospheric O_2/N_2 measurements at two Japanese sites: Estimation of global oceanic and land biotic carbon sinks and analysis of the variations in atmospheric potential oxygen (APO). *Tellus B: Chem. Phys. Meteorol.*, 60, 213–225, 2008.

Van der Laan–Luijkx, I. T., Van der Laan, S., Uglietti, C., Schibig, M. F., Neubert, R. E. M., Meijer, H. A. J., Brand, W. A., Jordan, A., Richter, J. M., Rothe, M., and Leuenberger, M. C.: Atmospheric CO_2, $\delta(O_2/N_2)$ and $\delta^{13}CO_2$ measurements at

1   Jungfraujoch, Switzerland: Results from a flask sampling intercomparison program, *Atmos. Meas. Tech.*, 6, 1805–1815,

2   2013.

3 Wieser, M.E., and Berglund, M.: Atomic weights of the elements 2007 (IUPAC Technical Report), *Pure Appl. Chem.*, 81,

4   2131–2156, 2009.

5 WMO: 18th WMO/IAEA Meeting on Carbon Dioxide, Other Greenhouse Gases and Related Tracers Measurement

6   Techniques (GGMT-2015), GAW Report, No. 229, 2016.

7 Zhao, C. L., Tan, P., and Thoning, K. W.: A high precision manometric system for absolute calibration of CO_2 in dry air, *J.*

8   *Geophys. Res.*, 102, 5885–5894, 1997.

1   Table 1. Isotopic composition and atomic masses of pure oxygen and pure nitrogen used to prepare highly precise O_2 standard

2   mixtures (HPOs).

Isotope	Atomic mass[a,b]	Isotope abundance		Isotopic ratio of source gas[e]
		Atmosphere[a]	Source gas[a]	
[14]N	14.0030740074(18)	0.996337(4) [c]	0.996346(4)	
[15]N	15.000108973(12)	0.003663(4) [c]	0.003654(4)	δ^{15}N = (−2.397 ± 0.001) ‰
[16]O	15.9949146223(25)	0.9975684(9)[d]	0.9975887(9)	
[17]O	16.99913150(22)	0.0003836(8)[d]	0.0003818(8)	δ^{17}O = (−4.66 ± 0.05) ‰
[18]O	17.9991604(9)	0.0020481(5)[d]	0.0020295(5)	δ^{18}O = (−9.075 ± 0.003) ‰
Sources	Atomic mass of nitrogen[a]		Atomic mass of oxygen[a]	
Atmosphere	14.006726(4)		15.999405(1)	
Source gases	14.006717(4)		15.999366(1)	

5   [a] Numbers in the parentheses represent the standard uncertainty in the last digits.

6   [b] Atomic mass and the standard uncertainty as determined by De Laeter et al. (2003).

7   [c] Abundance of the isotope and the standard uncertainty as determined using calculations for the absolute ^{15}N/^{14}N ratio

8   obtained by Junk and Svec (1958).

9   [d] Abundance of the isotope and the standard uncertainty were calculated using [17]O/[16]O = 12.08 ‰ and ^{18}O/[16]O = 23.88 ‰ vs.

10   the VSMOW as determined by Barkan and Luz (2005). The absolute isotopic ratio for VSMOW and the standard uncertainty

11   were determined by Li et al. (1988) for [17]O/^{16}O and Baertschi (1976) for ^{18}O/[16]O.

12   [e] Isotopic ratio is defined as the difference in the corresponding atmospheric value (AIST reference air) measured using a

13   mass spectrometer. Numbers following the symbol ± denote the standard uncertainty.
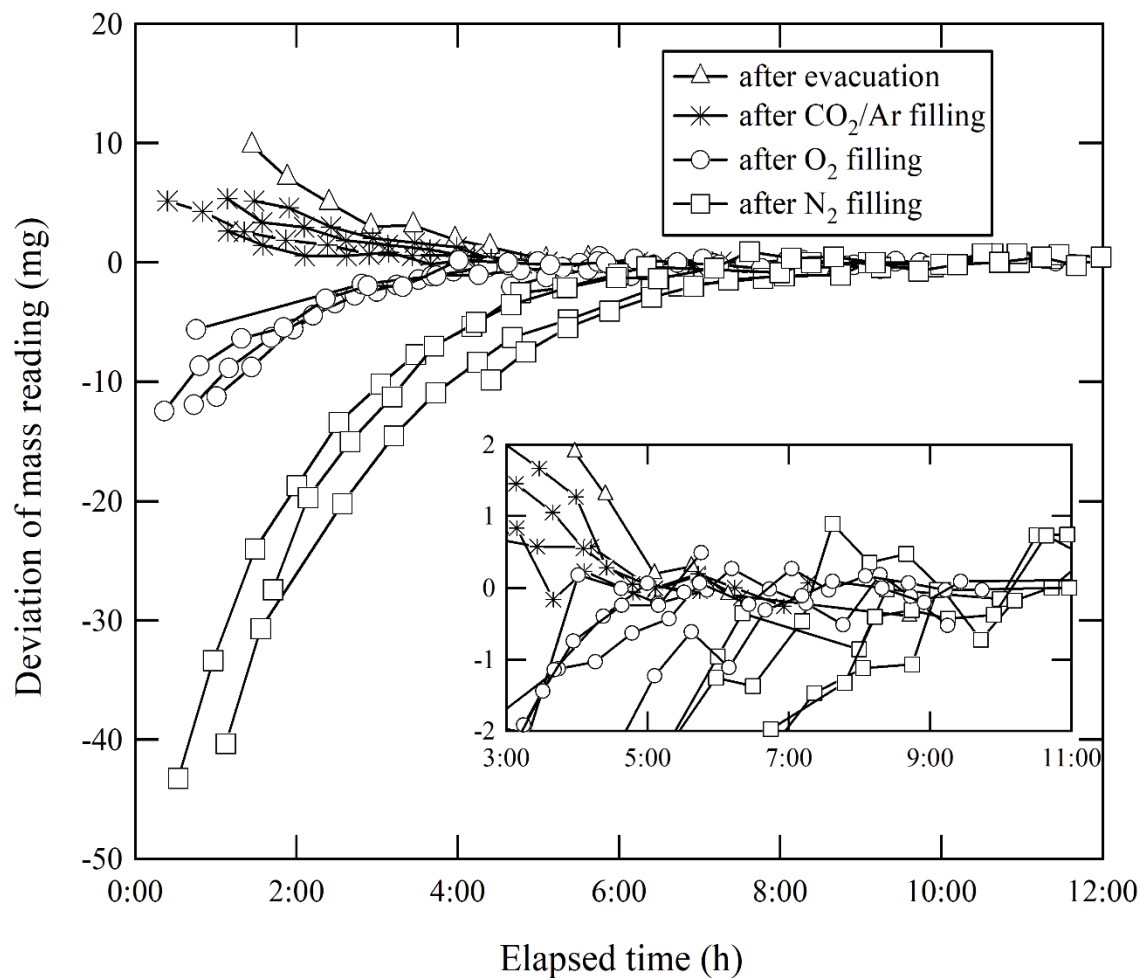
Figure 1 Changes in mass readings of sample cylinders plotted against the time elapsed after evacuation of the cylinder and filling of source gases. The mass readings were obtained using the weighing system. Deviation of the mass reading is expressed as the change in amount from the equilibrium value, which was defined as the mass reading when the standard deviation of the values remained constant for two or more hours.
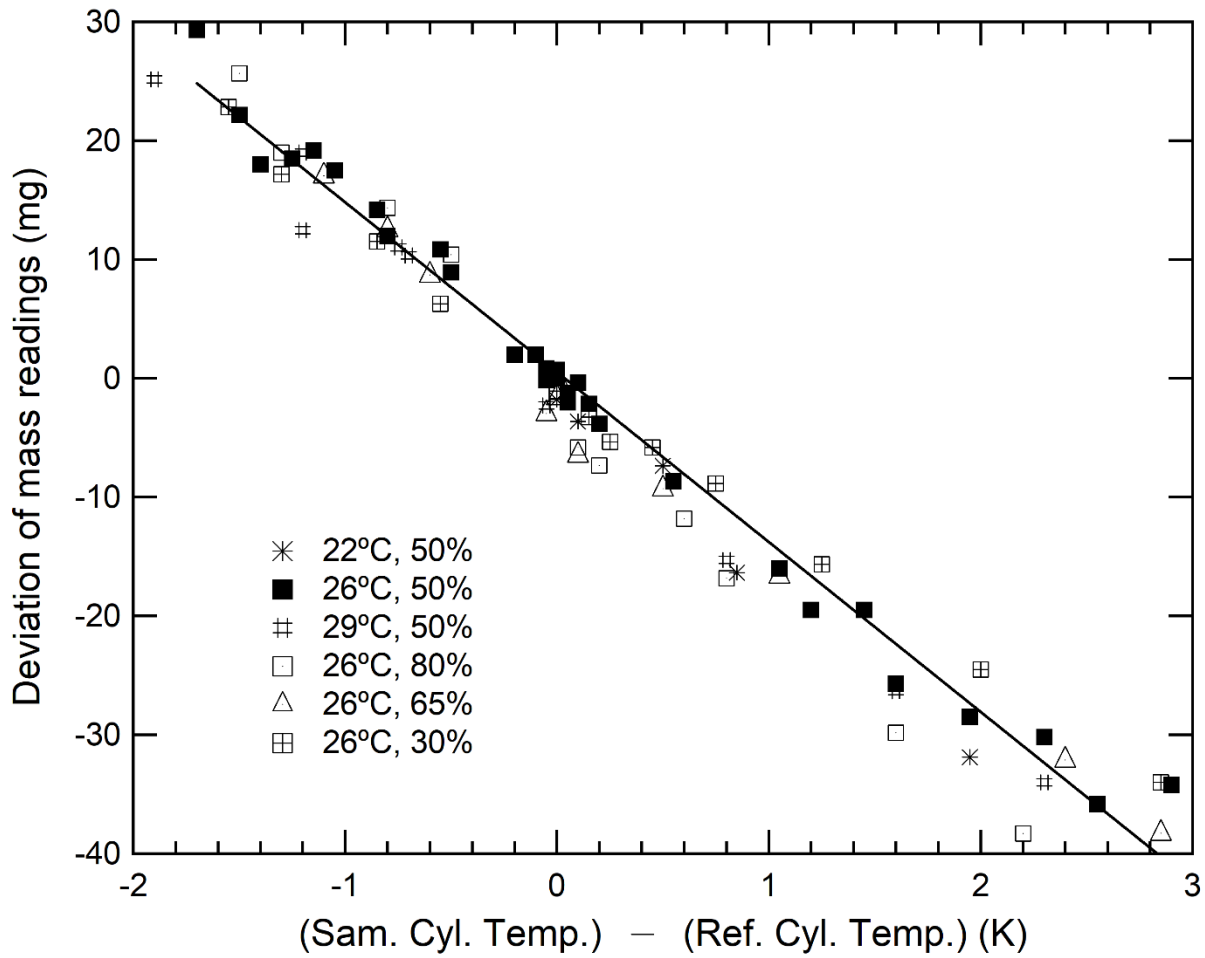
Figure 2 Changes in the mass readings observed for sample cylinders plotted against temperature differences obtained under various conditions (a temperature range from 22 ℃ to 29 ℃, a humidity range from 30% to 80%.)
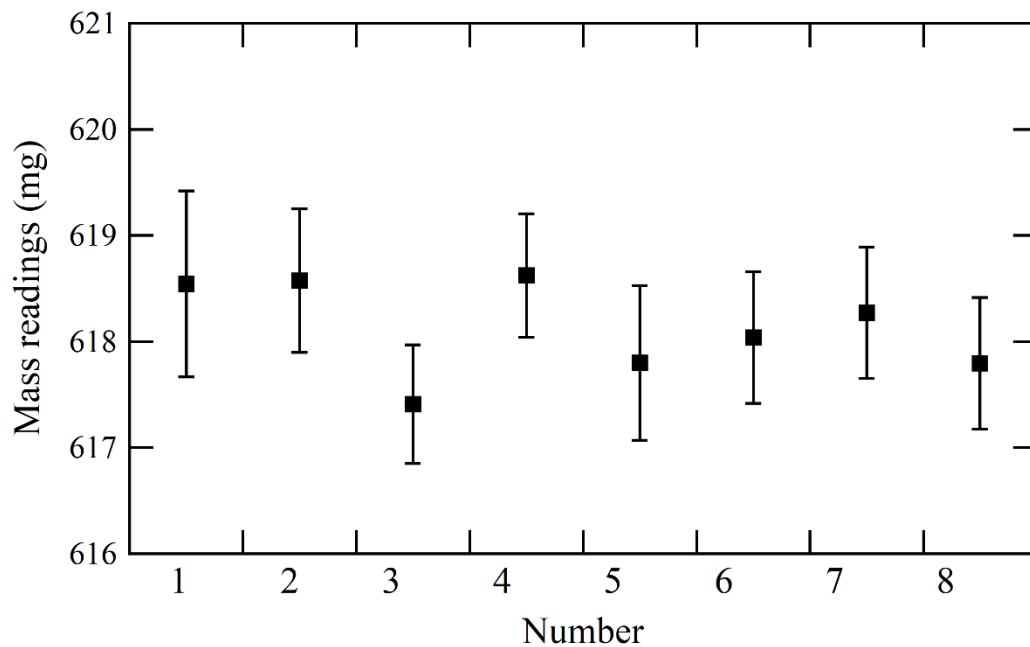
Figure 3 Reproducibility of mass readings obtained for the sample cylinder after cylinders had been heated at 40 ℃ (numbers 1 to 4) or cooled at 23 ℃ (numbers 5 to 8). The error bars represent the standard uncertainty.

Table 2. Gravimetric values of N_2, O_2, and CO_2 molar fractions alongside $(O_2/N_2)_{HPO\_grav}$, $(Ar/N_2)_{HPO\_grav}$, $\delta(O_2/N_2)_{HPO\_grav}$, and $\delta(Ar/N_2)_{HPO\_grav}$, as well as the measured values of CO_2 molar fractions in HPOs.

Cylinder number	Preparation date	Gravimetric values[a], μmol mol^{-1}								Measured values, μmol mol^{-1}
		N_2	O_2	Ar	CO_2	$(O_2/N_2)_{HPO\_grav}$	$(Ar/N_2)_{HPO\_grav}$	$\delta(O_2/N_2)_{HPO\_grav}$ [b]	$\delta(Ar/N_2)_{HPO\_grav}$ [b]	CO_2
CPC00556	15 March 2017	780094.1 ± 1.0	210068.3 ± 0.8	9415.2 ± 0.7	422.30 ± 0.03	0.2692858 ± 0.0000011	0.0120693 ± 0.0000009	4471.8 ± 4.0	9619 ± 77	422.37 ± 0.14
CPB28679	29 March 2017	782593.9 ± 0.8	207770.2 ± 0.7	9222.1 ± 0.6	413.64 ± 0.03	0.2654892 ± 0.0000009	0.0117841 ± 0.0000008	−9689.9 ± 3.4	−14244 ± 67	-
CPB16178	5 April 2017	779014.8 ± 1.0	211348.4 ± 0.8	9241.0 ± 0.7	395.78 ± 0.03	0.2713021 ± 0.0000010	0.0118624 ± 0.0000009	11993.0 ± 4.0	−7694 ± 77	395.96 ± 0.14
CPB16345	7 April 2017	781499.3 ± 1.0	208750.7 ± 0.8	9349.6 ± 0.7	400.43 ± 0.03	0.2671156 ± 0.0000011	0.0119636 ± 0.0000009	−3623.2 ± 4.0	777 ± 75	400.40 ± 0.14
CPB16315	12 April 2017	781264.1 ± 0.9	209040.6 ± 0.7	9297.0 ± 0.7	398.18 ± 0.03	0.2675671 ± 0.0000010	0.0118999 ± 0.0000009	−2595.1 ± 3.6	−5191 ± 79	398.21 ± 0.14
CPB16379	17 April 2017	781059.5 ± 0.8	209233.2 ± 0.7	9308.6 ± 0.6	398.68 ± 0.03	0.2678838 ± 0.0000009	0.0119179 ± 0.0000008	−757.9 ± 3.3	−3050 ± 65	398.68 ± 0.14
CPB16349	13 June 2017	780424.7 ± 0.8	209813.5 ± 0.7	9342.7 ± 0.6	419.06 ± 0.03	0.2688452 ± 0.0000009	0.0119713 ± 0.0000008	2828.5 ± 3.4	1419 ± 66	419.22 ± 0.14
CPB28912	15 June 2017	780792.3 ± 0.8	209437.0 ± 0.7	9351.1 ± 0.6	419.44 ± 0.03	0.2682366 ± 0.0000009	0.0119765 ± 0.0000008	558.1 ± 3.4	1851 ± 66	419.54 ± 0.14
CPB28679	22 June 2017	780869.0 ± 0.8	209383.9 ± 0.7	9328.6 ± 0.6	418.44 ± 0.03	0.2681421 ± 0.0000009	0.0119464 ± 0.0000008	205.8 ± 3.4	−664 ± 65	418.54 ± 0.14

[a] Numbers following the symbol ± denote the standard uncertainty.

[b] Values were calculated using the absolute O_2/N_2 and Ar/N_2 in AIST reference air as described in section 5.1.

Table 3. Typical contribution of each source of uncertainty (including the mass of the source gas, molar mass, and purity) to the standard uncertainties obtained for the molar fractions of N_2, O_2, Ar, and CO_2 in the HPO.

| Constituent | Uncertainty source, $\mu mol\ mol^{-1}$ | | | Combined standard uncertainty, $\mu mol\ mol^{-1}$ |
	Mass of source gas [a]	Molar mass [b]	Purity [c]	
N_2	0.77	0.11	0.05	0.77
O_2	0.63	0.03	0.03	0.63
Ar	0.56	0.13	0.02	0.58
CO_2	0.025	0.006	0.011	0.028

[a] The values were calculated in the procedure described in section 4.3.

[b] The values were calculated in the procedure described in section 4.2.

[c] The values were calculated in the procedure described in section 4.1.

Table 4. Impurities in source gases for preparation of HPOs

Impurity	Source gases, μmol mol^{-1}			
	CO$_2$	Ar	O$_2$	N$_2$
N$_2$	0.9 ± 0.5	0.12 ± 0.07	0.12 ± 0.07	-
O$_2$	0.3 ± 0.1	0.5 ± 0.3	-	0.05 ± 0.03
				0.05 ± 0.03
Ar	-	-	0.089 ± 0.052	0.28 ± 0.01
				0.32 ± 0.03
CO$_2$	-	0.002 ± 0.001	0.124 ± 0.004	0.002 ± 0.001
H$_2$O	4.8 ± 2.7	0.05 ± 0.03	0.05 ± 0.03	0.05 ± 0.03
CH$_4$	0.6 ± 0.3	0.005 ± 0.003	0.005 ± 0.003	0.005 ± 0.003
CO	-	0.04 ± 0.02	0.04 ± 0.02	0.04 ± 0.02
H$_2$	2.2 ± 1.3	-	-	-
				999999.8 ± 0.1
Purity	999991.3 ±3.1	999999.3 ± 0.3	999999.6 ± 0.1	999999.6 ± 0.1
				999999.5 ± 0.1

Numbers following the symbol ± denote the standard uncertainty.

"-" represents the constituents which were not measured.
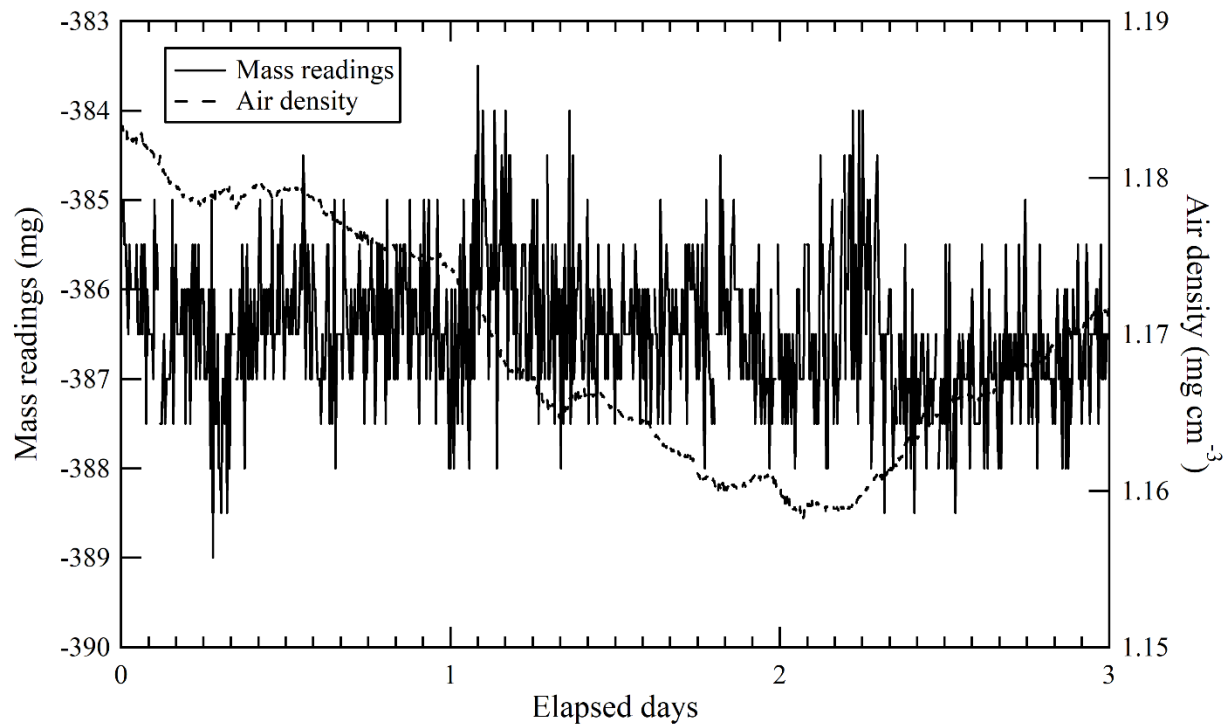
Figure 4 Repeatability of mass readings obtained for the sample cylinders and ambient air density for three days. Solid and dashed lines represent mass readings and ambient air density, respectively

Table 5. $\delta(^{15}N^{14}N/^{14}N^{14}N)_{HPO\_meas}$, $\delta(^{17}O^{16}O/^{16}O^{16}O)_{HPO\_meas}$, $\delta(^{18}O^{16}O/^{16}O^{16}O)_{HPO\_meas}$, $\delta(^{16}O^{16}O/^{14}N^{14}N)_{HPO\_meas}$, $\delta(^{36}Ar/^{40}Ar)_{HPO\_meas}$ and $\delta(^{40}Ar/^{14}N^{14}N)_{HPO\_meas}$ measured by the mass spectrometer. $\delta(O_2/N_2)_{HPO\_meas}$ and $\delta(Ar/\ N_2)_{HPO\_meas}$ calculated using equations (3) and (4), and differences between $\delta(O_2/N_2)_{HPO\_meas}$ and $\delta(^{16}O^{16}O/^{14}N^{14}N)_{HPO\_meas}$ are also shown.

Cylinder number	$\delta(^{15}N^{14}N/^{14}N^{14}N)_{HPO\_meas}$	$\delta(^{17}O^{16}O/^{16}O^{16}O)_{HPO\_meas}$	$\delta(^{18}O^{16}O/^{16}O^{16}O)_{HPO\_meas}$	$\delta(^{16}O^{16}O/^{14}N^{14}N)_{HPO\_meas}$	$\delta(O_2/N_2)_{HPO\_meas}$	$\delta(O_2/N_2)_{HPO\_meas} - \delta(^{16}O^{16}O/^{14}N^{14}N)$	$\delta(^{36}Ar/^{40}Ar)_{HPO\_meas}$	$\delta(^{40}Ar/^{14}N^{14}N)_{HPO\_meas}$	$\delta(Ar/N_2)_{HPO\_meas}$
CPC00556	−2365.0 ± 1.2	−4032 ± 50	−7907.8 ± 2.6	4477.5 ± 3.2	4459.2 ± 3.2	−18.2	−2465 ± 50	9649.0 ± 6.5	9658.1 ± 6.5
CPB28679	−2343.5 ± 1.2	−4032 ± 50	−8298.0 ± 2.6	−9704.7 ± 3.2	−9724.4 ± 3.2	−19.7	−1969 ± 50	−14102.6 ± 6.5	−14092.2 ± 6.5
CPB16178	−2372.5 ± 1.2	−4219 ± 50	−8279.7 ± 2.6	12011.7 ± 3.2	11991.7 ± 3.2	−20.0	−2197 ± 50	−7828.0 ± 6.5	−7818.1 ± 6.5
CPB16345	−2351.5 ± 1.2	−4676 ± 50	−9087.6 ± 2.6	−3624.2 ± 3.2	−3647.7 ± 3.2	−23.5	−2311 ± 50	712.0 ± 6.5	721.5 ± 6.5
CPB16315	−2356.2 ± 1.2	−4665 ± 50	−9069.6 ± 2.6	−1946.8 ± 3.2	−1970.2 ± 3.2	−23.4	−2228 ± 50	−4538.2 ± 6.5	−4528.5 ± 6.5
CPB16379	−2416.8 ± 1.2	−4655 ± 50	−9062.8 ± 2.6	−763.6 ± 3.2	−786.6 ± 3.2	−22.9	−2261 ± 50	−3074.4 ± 6.5	−3064.3 ± 6.5
CPB16349	−2407.9 ± 1.2	−4630 ± 50	−9036.0 ± 2.6	2833.1 ± 3.2	2810.2 ± 3.2	−23.0	−2360 ± 50	1485.7 ± 6.5	1495.4 ± 6.5
CPB28912	−2397.2 ± 1.2	−4656 ± 50	−9075.3 ± 2.6	554.6 ± 3.2	531.5 ± 3.2	−23.2	−2348 ± 50	1812.2 ± 6.5	1821.9 ± 6.5
CPB28679	−2390.8 ± 1.2	−5109 ± 50	−9941.2 ± 2.6	212.5 ± 3.2	185.4 ± 3.2	−27.1	−2338 ± 50	−642.8 ± 6.5	−633.2 ± 6.5

These values are on the AIST scale, i.e., determined against AIST reference air and are given in per meg.

Numbers following the symbol ± denote the standard uncertainty.
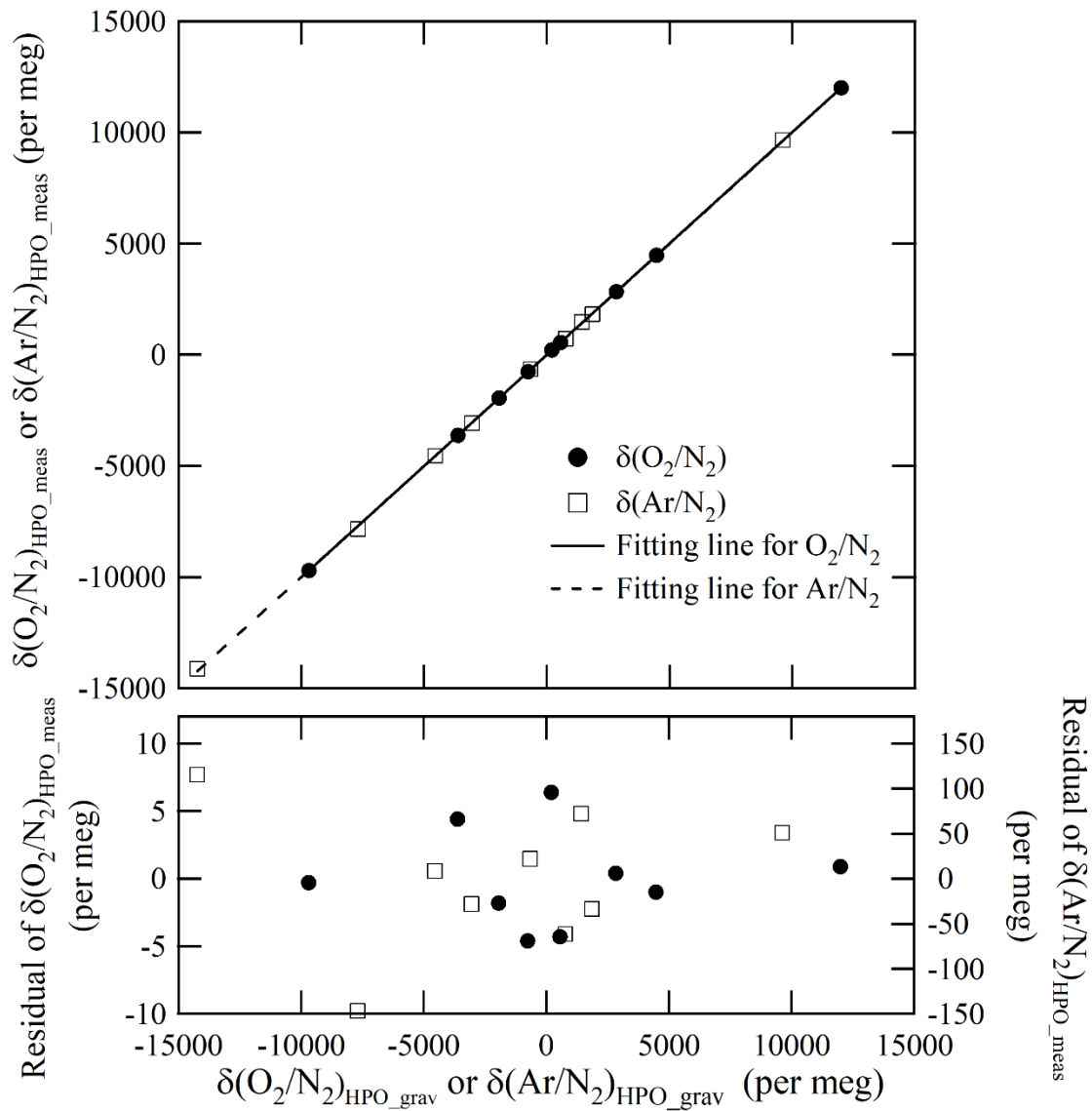
Figure 5 Relationship between $\delta(O_2/N_2)_{HPO\_grav}$ and $\delta(Ar/N_2)_{HPO\_meas}$ on the AIST scale (upper). Fitting residuals $\delta(O_2/N_2)_{HPO\_meas}$ and $\delta(Ar/N_2)_{HPO\_meas}$ are likewise shown (lower).